AWARD NUMBER: W81XWH-10-1-0543

TITLE: Biomarkers in the Detection of Prostate Cancer in African Americans

PRINCIPAL INVESTIGATOR: William E. Grizzle, Ph.D.

CONTRACTING ORGANIZATION: University of Alabama at Birmingham
Birmingham, AL 35294

REPORT DATE: September 2014

TYPE OF REPORT: Annual

PREPARED FOR: U.S. Army Medical Research and Materiel Command
Fort Detrick, Maryland 21702-5012

DISTRIBUTION STATEMENT: Approved for Public Release;
Distribution Unlimited

The views, opinions and/or findings contained in this report are those of the author(s) and should not be construed as an official Department of the Army position, policy or decision unless so designated by other documentation.

REPORT DOCUMENTATION PAGE

Form Approved
OMB No. 0704-0188

Public reporting burden for this collection of information is estimated to average 1 hour per response, including the time for reviewing instructions, searching existing data sources, gathering and maintaining the data needed, and completing and reviewing this collection of information. Send comments regarding this burden estimate or any other aspect of this collection of information, including suggestions for reducing this burden to Department of Defense, Washington Headquarters Services, Directorate for Information Operations and Reports (0704-0188), 1215 Jefferson Davis Highway, Suite 1204, Arlington, VA 22202-4302. Respondents should be aware that notwithstanding any other provision of law, no person shall be subject to any penalty for failing to comply with a collection of information if it does not display a currently valid OMB control number. **PLEASE DO NOT RETURN YOUR FORM TO THE ABOVE ADDRESS.**

1. REPORT DATE	2. REPORT TYPE	3. DATES COVERED
September 2014	Annual	1 Sep 2013 –31 Aug 2014

4. TITLE AND SUBTITLE

Biomarkers in the Detection of Prostate Cancer in African Americans

5a. CONTRACT NUMBER

5b. GRANT NUMBER
W81XWH-10-1-0543

5c. PROGRAM ELEMENT NUMBER

6. AUTHOR(S)
Dr. William E. Grizzle and Dr. Sandra M. Gaston

E-Mail: wgrizzle@uab.edu / sgaston@tuftsmedicalcenter.org

5d. PROJECT NUMBER

5e. TASK NUMBER

5f. WORK UNIT NUMBER

7. PERFORMING ORGANIZATION NAME(S) AND ADDRESS(ES)

University of Alabama at Birmingham

Birmingham, AL 35294-0007

8. PERFORMING ORGANIZATION REPORT NUMBER

9. SPONSORING / MONITORING AGENCY NAME(S) AND ADDRESS(ES)
U.S. Army Medical Research and Materiel Command
Fort Detrick, Maryland 21702-5012

10. SPONSOR/MONITOR'S ACRONYM(S)

11. SPONSOR/MONITOR'S REPORT NUMBER(S)

12. DISTRIBUTION / AVAILABILITY STATEMENT
Approved for Public Release; Distribution Unlimited

13. SUPPLEMENTARY NOTES

14. ABSTRACT

This grant focuses on identifying molecular features of prostatic adenocarcinomas (PrCa) from African Americans (AAs) which we hypothesize may differ from the molecular features of PrCas from European Americans (EAs). Of note are those molecular characteristics which may be associated with aggressiveness of PrCas; hence, the differential expression of molecules may, in part, explain why AAs tend to have more aggressive PrCa than EAs. Also, we hypothesize that PrCas generate localized field effects that modify molecularly uninvolved prostate glands even though they appear to be histopathologically normal and unchanged. The field effects may vary with distance from foci of PrCa and may include epigenetic silencing of specific genes. Because AAs more frequently select radiation instead of radical surgery, less tissues have been available to study PrCa in AAs. Thus, this project uses nitrocellulose blots (tissue prints) of biopsies of the prostate as a source of RNA, DNA and proteins to identify molecular features of PrCas and of uninvolved prostate glands that differ racially. In addition, racial admixtures based on single nucleotide polymorphisms (SNPs) are used to define more accurately the racial ancestry of patients.

15. SUBJECT TERMS
Prostate cancer, molecular markers, multiplex immunoassays, racial differences

16. SECURITY CLASSIFICATION OF:			17. LIMITATION OF ABSTRACT	18. NUMBER OF PAGES	19a. NAME OF RESPONSIBLE PERSON
a. REPORT	b. ABSTRACT	c. THIS PAGE			USAMRMC
U	U	U	UU	49	19b. TELEPHONE NUMBER *(include area code)*

Table of Contents

INTRODUCTION

African Americans (AAs) who have prostatic adenocarcinomas (PrCas) tend to have poorer outcomes, overall, than European Americans (EAs) who have equivalent PrCas. The causes of this poorer prognosis are not understood. In addition, the molecular features of PrCa that may vary among AAs and EAs with PrCa have not been identified adequately. The underlying hypothesis of these grants is that molecular characteristics of PrCas vary with race and such molecular differences may explain the more aggressive behavior of PrCas of AAs compared to equivalent PrCas of EAs. Of note, molecular features and/or their transduction pathways may be targets, in the future, for molecularly based therapies. Thus, a major goal of these grants is to characterize potentially aggressive molecular features of PrCas from AAs that differ from molecular features of equivalent PrCas from EAs.

Another hypothesis that may explain differences in outcomes of PrCa based on race, is that PrCas may induce local field effects that affect uninvolved prostate glands and that these field effects may vary with race and the Gleason score of the PrCa. Such field effects have been described for the adenomatous polyposis coli (APC) gene, the glutathione S transferase-p1 (GSTp1) gene and RASSFIA, a putative tumor suppressor gene. Our findings that human epididymis protein-4 (HE4) is decreased in the serum of patients with PrCa compared to serum of patients evaluated for PrCa but with negative biopsies may be caused by similar field effects via hypermethylation of the promoter of WFDC2, the gene of HE4.

The first approach is to identify molecular features of PrCas that are different between PrCas and matching uninvolved histopathologically normal appearing prostate glands from the same cases. Subsequently, the molecular markers that are different between PrCas and uninvolved prostate glands in AAs will be compared with those from EAs. These molecular features will be evaluated with a focus on those molecules that are likely to be associated with the aggressiveness of PrCas.
Because AAs frequently select therapy by radiation rather than radical surgery, less tissue has been available to study. PrCa in AA patients. In addition, patients with PrCas with higher stage and Gleason scores are sometimes not candidates for radical surgery, independent of race. To improve the study of PrCa in these categories for which tissues are limiting to research, we obtain and utilize nitrocellulose (NC) blots (tissue prints) of prostate biopsies. Specifically, NC blots are obtained from all prostate biopsies of a case (i.e., patent evaluated for PrCa). Total RNA, DNA and proteins are extracted from NC blots of selected biopsies based on the presence or absence of PrCa in individual biopsies. Analyses of these extracts are at various molecular levels, e.g., epigenetically regulated (methylated) promoters of genes at the DNA level. Also, the mRNA and microRNA levels and protein levels can be analyzed. For example, the mRNA extracted from nitrocellulose blots is analyzed on the Affymetrix platform at the core facility of Harvard Medical School to identify mRNAs associated with PrCa. This discovery approach is confirmed by RTQ-PCR in a different set of samples with PrCa. Separately, the methylation of DNA is analyzed focusing on those genes, GSTp1, APC, RASSF1A, and WFDC2, for which preliminary results indicate that hypermethylation field effects are induced by foci of PrCa. Proteins identified to be differentially expressed in patients with and without PrCa are analyzed in serum, plasma, and urine by multiplex ((Luminex (BioPlex)) and in PrCa versus matched uninvolved prostate glands by liquid chromatography mass spectrometry and by immunohistochemistry. Based on the discovery results, results are confirmed in different sets of samples.

BODY

Administrative: In 2014, the major administrative issues were the renewal of IRBs at UAB and UCA. Because the collection of the contracted 60 cases of PrCa was successfully completed at UCA, the IRB at UCA is now in the data analysis only category and no further cases are being accrued.

During 2014, several new personnel joined our project. These included two new urologists, Drs. J. Nix and Soroush Rais-Bahrami, a new urologic pathologist, Dr. J. Gordetsky, a new postdoctoral fellow, Dr. D. Otali, and a new technician, Ms. A. Stewart. Dr. Nix, Dr. Otali and Ms. Stewart have been added by amendment to the UAB IRB of this project. We have submitted an amendment to add Drs. Soroush Rais-Bahrami and J. Gordetsky to the IRB.

During 2014, Dr. J. Nix, a new urologist at UAB joined our grant as a collaborator. Both he and Dr. Soroush Rais-Bahrami specialize in using overlays of magnetic resonance imaging (MRI) over real time ultrasound images (MRI-US)

to identify suspicious (atypical) areas of the prostate that are likely to harbor foci of PrCa. This adds critical technology to our study of the field effects induced by foci of prostate cancer.

In 2014, Dr. Grizzle continued to be a consultant to the DOD Prostate Cancer Tissue Repository. In addition, he continued as a participating member of the External Advisory Committee of the DOD Repository of Lung Cancer. Both these activities have ended or are in the tissue distribution phases and no additional patients are being accrued. Dr. Grizzle is still available for consultation to these activities.
In 2014, Dr. Gaston has served on the NCI Special Emphasis Panels for the review of grant applications for Cancer Genetics and Innovative Technologies for Cancer Research. During this last year, Dr. Gaston served as a reviewer for the DOD Prostate Cancer Research Program (Detection Diagnosis and Prognosis Peer Review Panel).

Specific Scientific Progress and Results:

Collection of Nitrocellulose Blots for Analysis: In this last reporting period, 66 study subjects were enrolled for gene expression studies for a cumulative enrollment of 117 patients, 83 AA and 34 EA. Specifically, nitrocellulose blots (i.e., tissue prints) were obtained from each of the diagnostic prostate biopsy cores obtained primarily via ultrasound (US) guidance on these cases. To date, prostate biopsy tissue samples from all study subjects have been transferred to Dr. Gaston's laboratory. Based on 12 nitrocellulose blots on each case, this results in 996 nitrocellulose blots from AAs and 408 NC blots from EAs. The details of the pathology diagnosis are outlined in Tables 1 and 2. Overall, 46% of our study subjects were diagnosed with prostate cancer, 21% with high grade prostate cancer (Gleason sum score 7 or more) and 25% with low grade prostate cancer (Gleason sum 6). In our AA and EA study subjects, the % cancer diagnosis, % high grade cancer and % low grade cancer were very similar.

In this reporting period, a new technology of obtaining biopsies using magnetic resonance imaging fused with active ultrasound (MRI-US) has been incorporated into the studies. MRI-US identifies areas suspicious for PrCa based on molecular effects identified by this technology. The suspicious areas are sampled by biopsy much more intensively than non-suspicious areas but non-suspicious areas also are biopsied using standard systematic approaches. The biopsies obtained by MRI-US are nitrocellulose (NC) blotted just as with standard US directed biopsies. The addition of this technology to our project is permitted by obtaining the MRI-US equipment and the addition of two faculty members, Dr. Jeffrey Nix and Dr. Soroush Rais-Bahrami, both of whom have extensive experience in using this methodology, and support of a radiologist, Dr. John V. Thomas, who is also trained in this technology. MRI-US biopsies are more likely to have PrCa and/or uninvolved prostate glands closely adjacent to PrCa than systematic biopsies obtained by US. Thus, such samples should provide more information on the PrCa as well as the interaction of PrCa with closely adjacent uninvolved prostate glands. In this reporting period, biopsies from 2 EA and 1 AA were obtained by this MRI-US technology.

Most features of sporadic cancer are not directly caused by differences in the germ line genomic sequences. Although different patterns of single nucleotide polymorphisms (SNPs) may increase the risk for developing specific cancers; instead epigenetic regulation by promoter methylation of gene expression of specific proteins and the post-transcriptional regulation of molecular features that affect the development and progression of PrCa are more important (McNally et al 2013, Grizzle et al 2011). One focus in these studies is on small and large non-translateable RNAs that, for example, may regulate mRNAs either to increase or to decrease the phenotypic expression of specific proteins.

Analysis of Epigenetic DNA Hypermethylation Field Effect Biomarkers

During this last year, we completed an important study in which tissue prints of diagnostic prostate biopsies were used to determine if the field effects generated by cancer-associated DNA methylation might serve as a useful test for the presence of occult prostate cancer in the tissues adjacent to the biopsy core. Many studies have shown that tumor-associated changes in DNA methylation can act as biomarkers for the presence of prostate cancer. We have identified three DNA hypermethylation markers (GSTp1, APC and RASSF1A) with field effects that extend far enough around the histological boundary of a prostate cancer focus to be detected in a biopsy core several millimeters away. Importantly, we found that both the magnitude and the extent of field-effect hypermethylation are sensitive to the grade of the adjacent prostate cancer. To ensure that this study included enough African American subjects to determine if this field effect test could be used in this high risk population, we included a set of study subjects from Alabama as well as from New England.

Tissue prints were prospectively collected from biopsy cores from study subjects undergoing diagnostic prostate biopsies. DNA from all 12 cores was analyzed for the DNA hypermethylation markers glutathione-S-transferase p 1 (GSTP1), adenomatous polyposis coli (APC) and ras association domain family member 1 (RASSF1). Levels of hypermethylation are reported relative to a reference gene, beta actin (ACTB). We compared three groups of patients:

Group 1 (Controls): All 12 cores negative for cancer and for high grade PIN, no suspicious histology.

Group 2: Biopsies show a limited amount of low grade (Gleason 3+3) prostate cancer.

Group 3: At least 1 of 12 cores positive for higher Grade (Gleason 7 or greater) prostate cancer

(See Field Effect Study Overview – Figure 1)

We observed a statistically significant increase in field effect hypermethylation **in the histologically benign cores** from control (group 1) to group 2 to group 3 for each of the three markers (table 3). This observation suggests that this epigenetic change in the benign tissue surrounding a prostate cancer is sensitive to the Gleason grade of the tumor. The level of hypermethylation in the cancer cores also shows correlation with Gleason grade. Interestingly, the level of hypermethylation is biopsy cores with Gleason 6 prostate cancer shows a different pattern in Group 2 (only Gleason 6 in the gland) than in Group 3 (also some higher grade cancer elsewhere in the gland). See Table 4 and Figure 2.

This prototype "field effect" test is particularly timely as more patients are asked to consider active surveillance rather than immediate treatment based on a biopsy diagnosis of low grade prostate cancer. We note that published studies report that for several DNA markers the extent of hypermethylation is higher in prostate cancers from AAs than EAs and an initial review of GSTp1, APC and RASSF1 markers in a small group of self-identified AA patients suggests that the extent of field effect hypermethylation may be more extensive (more cores involved) than in similar EA patients. Inasmuch as our plan of work for DOD project PC093309 already calls for the preparation of DNA samples for the analysis of ancestry informative markers, we plan to use a new set of AA and EA study subjects from the Birmingham Alabama area for validation studies to further confirm these findings.

Field effects of PrCa on adjacent uninvolved prostate glands: Our data indicate that mRNA for the adenomatous polyposis coli gene (APC), the gene, glutathione S-transferase p1 (GSTp1), and the putative suppressor gene, RASSFIA, are suppressed in uninvolved prostate glands associated with cases with PrCa. The extent of suppression of these genes in uninvolved prostate glands is thought to increase the Gleason core of the PrCa. During this reporting period, we used immunohistochemistry to evaluate whether the suppression of genes resulted in decreased phenotypic expression of protein in the uninvolved glands adjacent to PrCa.

For the gene GSTp1, the GSTp1 protein was not detected in PrCa in 18 of 20 cases that were evaluated as demonstrated in Figure 3.

For uninvolved glands, the staining of GSTp1 was strongest in the basal cells, in which the most prominent staining was nuclear with slightly less staining of the cytoplasm. There was less staining of the luminal cells in which most staining was weak to moderate with nuclear and cytoplasmic about equivalent, but with slightly stronger membranous and perinuclear staining. In general, the staining of the uninvolved glands for GSTp1 was quite variable and the lower staining of uninvolved glands adjacent to PrCa but this was not always consistent; however, the difference in GSTp1 staining between uninvolved glands adjacent to PrCa and away from PrCa was much less than would be expected based upon downregulation of the gene for GSTp1.

All 20 cases of PrCa stained weak to moderately for APC as is demonstrated in Figure 4. For the uninvolved prostate glands, there was not as clear a difference in staining of luminal versus basal cells as was noted for GSTp1. The strongest staining in both basal and luminal cells was perinuclear followed by staining of the cellular membrane. There was less staining of the cytoplasm. While in general the staining for APC in the uninvolved gland adjacent to PrCa, as with GSTp1, was somewhat less, the difference was small and conclusions were difficult to make as to suppression of protein expression by PrCa.

Multiplex (Luminex, Bioplex) Immunoassays: The Luminex (BioPlex) technology of immunoassays permit concomitant assays of up to 100 individual molecules on one specimen and approximately 34 specimens can be analyzed in duplicate in the same assay. Immunoassays of cytokines and tumor biomarkers can utilize serum, plasma, urine, as well as lysates of cells and tissue. Our prior results comparing serum and plasma found that most molecules are higher in plasma than in serum. Unexpectedly, in most cases, the cytokines in plasma were lower in patients with PrCa than in patients suspected of having PrCa due to of elevated prostate specific antigen (PSA) in serum but without PCa on biopsy.

Our efforts to identify racial differences in PrCa using Luminex (i.e., Bioplex) technology has been challenging because only patients who are being evaluated for PrCa are included in the study. There are no normal controls because such comparisons do not represent a realistic medical evaluation because young individuals and individuals without elevated PSA are seldom evaluated for PrCa.

Our study consists of two groups – one with PrCa identified by biopsy and the control group who do not have PrCa based on biopsy. Patients identified to have high grade PIN and/or with histories of other malignancies are excluded from both groups; however, there remains the problem that patients in whom PrCa was not identified on biopsy still may harbor PrCa that was missed on biopsy and is indolent or is progressing slowly. In each study, we determine the current status of patients without PrCa, if available from the medical record. Also, some patients in both groups may have undiagnosed malignancies when samples were obtained.

In our initial review of levels of cytokines and tumor biomarkers in serum and plasma from patients with PrCa and cases evaluated for PrCa in which no PrCa was found on biopsy, we identified that human epididymis protein-4 (HE4) was greatly decreased in patients with PrCa compared to patients in whom no PrCa was identified in standard prostate biopsies (Figure 5). Because PrCa seldom replaces most of the uninvolved glands of the prostate, lower blood levels in patients with PrCa is most consistent with decreased HE4 in the uninvolved glands of patients with PrCa.

Of note, HE4, encoded by the WFDC2 gene, is a secreted glycoprotein whose expression is restricted in most normal tissues but is usually associated with expression in the reproductive tract where it has been found to be important in the maturation of sperm but also is likely to have other functions, especially in females. In contrast to the results in prostate cancer, high levels of expression HE4 is indicative of a diagnosis of ovarian papillary serous and ovarian endometriod carcinomas (about 90% of patients express high levels of HE4) and/or the recurrence of these cancers following therapy; HE4 also is increased in patients with endometrial cancers. These results have a very strong association with these cancers so they have been accepted by the FDA as diagnostically useful for monitoring ovarian carcinomas.

In contrast to ovarian and endometrial cancers, our results demonstrated decreased levels of HE4 in the serum of patients with PrCa compared to patients without PrCa. This confusing result led to our study of HE4 based on the literature, immunohistochemistry and mass spectrometry. Our interest was based upon the hypothesis that HE4 might be from a gene hypermethylated by a field effect induced by PrCa similar to that seen in GSTp1. Alternatively, HE4 might be only apparently decreased due to some type of bias. For example, the lower levels could be secondary to the decay of HE4 on storage of samples. Similar sample effects have been reported for cytokines in serum samples from patients with melanomas stored for more than just 2 to 3 years (Potter et al 2012).

The literature indicates that in contrast to serum from ovarian carcinomas, the mRNA of HE4 (WFDC2) in tissues of PrCa is strongly decreased compared with HE4 in uninvolved prostate glands (Kim et al 2011).

Consistently, the literature indicates that the WFDC2 promoter is frequently methylated in cancer (17/22 and 6/6 malignant cell lines) but not in normal prostate tissue (0/10, or the normal PrCa cell line) (Kim et al 2011). The methylation of WFDC2 in uninvolved prostate glands adjacent to PrCa has not been adequately evaluated; however, it has been suggested it may be similar to GSTp1, and hence, suppress HE4 in adjacent uninvolved glands.

We also have performed immunohistochemistry on prostate tissues from radical prostatectomies with PrCa and prostate tissues from radical cystectomy specimens without PrCa. Staining of PrCa was compared to staining of uninvolved matching prostate glands, both from radical prostatectomies and benign prostatic hyperplasia and normal prostate glands from radical cystectomy specimens. Immunostaining of a case with PrCa is demonstrated in Figure 6. This pattern of HE4 staining is typical for all the 20 cases of PrCa evaluated by immunohistochemistry. The immunostaining indicates that HE4 is expressed in PrCa in the perinuclear area, the cytoplasm and the cell membranes. In the uninvolved prostate glands in cases with PrCa, HE4 is most strongly expressed in the basal cell in the same general intracellular pattern as

described for PrCa. When prostates removed in a radical cystectomy operation in which there is no PrCa were identified were immunostained for HE4, the corpora amylacea stained moderately to strongly for HE4 (Figure 7). This would be consistent with the secretion of the HE4 and the incorporation of this glycoprotein into the corpora amylacea.

Of note, the cells of PrCa stained at about the same intensity as the basal cells of uninvolved glands (Figure 6). We next began an evaluation of the expression of HE4 by mass spectrometry in macrodissected PrCa and matching uninvolved glands.

Discovery of proteins in PrCa using mass spectrometry: In 2014, we continued to work with our collaborator, Dr. James Mobley, who heads the proteomics facility of the UAB Comprehensive Cancer Center. This core contains cutting edge mass spectrometry instrumentation (e.g., a Hybrid Orbitrap Velos Pro mass spectrometry system (Thermo) with an in line sampler from Agilent)). Specifically, this latest instrumentation of mass spectrometry will be used to survey the global proteome extracted from the clinical prostate specimens (frozen, FFPE, and bodily fluids). This system can identify from protein digests more proteins than any other system on the market (about 2000). Our preliminary studies have confirmed that as small as 1μg of protein extracts from paraffin embedded tissues, frozen and fresh tissues, as well as bodily fluids can be analyzed by this system. Extracted proteins from such samples and digested and cleaved by trypsin are separated using a 20 cm X 75 micrometer in side diameter column that separates the peptide/digested fragments based on a 3 hour gradient. Data analysis incorporates the Refine MS from gene data as well as other local data analysis systems.

In 2014, we found that paraffin embedded biopsies of our cases could not be utilized for discovery analysis based on mass spectrometry without compromising the diagnostic material. Thus, for our initial discovery studies, we shifted to using macrodissected PrCa and matching uninvolved prostate glands from radical prostatectomies. In our pilot study, PrCa and uninvolved prostate glands macrodissected samples from 8 AA patients and 12 paired macrodissected PrCa and uninvolved prostate gland samples from EA patients were extracted, processed and prepared to run on the Hybrid Orbitrap Velos Pro system. Our initial focus was to be on the molecules SFASL, EGF, CEA, IL-13, G-CSF and MIP-1β which previously were found to be elevated in both the serum and plasma from patients confirmed by biopsy to have had PrCa when samples were compared to the control group. Of less interest are those molecules previously found by our BioPlex studies to be decreased in serum and plasma from PrCa cases compared to controls including HE4, il-1a, il-1b, il6, and il-8.

Our initial mass spectrometry evaluation of paired macrodissected PrCa and uninvolved prostate glands from 8 AA and 12 EA patents (40 samples total), identified that more protein was required for optimal analysis by mass spectrometry than could be extracted from the unstained sections provided to the proteomic laboratory in many of these cases. Successful data from MS were obtained from 4 EA pairs of specimens and from 5 AA pairs of specimens. Evaluation of the protein extraction indicated that extraction of protein from paraffin embedded tissues is much less efficient than extraction of protein from frozen tissues and some of the extracted material caused problems with the mass spectrometry system (e.g., caused loss of sensitivity of detectors requiring frequent cleaning of the MS system). On the cases for which inadequate protein was extracted, additional paraffin sections have been provided to the Proteomic Core and proteins are now being extracted from the new samples. These results confirmed our view that paraffin embedded **biopsies cannot be used** in these discovery studies. For adequate data analysis from the specimens, it is optimal to analyze the MS data on all specimens together. Thus, we are waiting until the 8 additional EA cases and 4 additional AA cases are extracted and successfully run on the mass spectrometry instrumentation.

Gene Profiling Studies

Affymetrix Whole Transcriptome mRNA Gene Expression Profiling:

This year, we have successfully used Affymetrix HTA 2.0 arrays to analyze gene expression profiles of tissue-print RNA obtained from biopsies from AA and EA men who were diagnosed with high volume, high grade prostate cancer. This is an important project milestone that addresses a significant disparity in the representation of AA patients with high grade disease in prostate cancer gene expression datasets. Patients with extensive high grade cancer on biopsy are usually treated by hormonal therapy and/or radiation, not surgically, and as a result only biopsy tissue is available for biomarker studies. Moreover, in the Birmingham area as in many other parts of the country, AA patients are more likely to choose radiation over surgery for prostate cancer treatment, which has further limited the representation of AA in biorepository collections that depend on radical prostatectomy specimens.

We have chosen to use the Affymetrix Human Whole Transcriptome Array 2.0 as the most up to date and appropriate expression array for our biomarker discovery studies. Our strategy for the whole transcriptome-discovery study is illustrated in Figure 8. For our AA and EA study groups diagnosed with high grade prostate cancer, we are focusing on subjects with biopsy cores that contain 50% or more high-grade carcinoma. Our study design compares RNA expression profiles from high grade and high % cancer cores with RNA from tumor-adjacent cores from the same prostate that are not involved with cancer (or with the least involved core, if all cores are cancer-positive). Also, we are also comparing RNA expression from our subjects with high grade prostate cancer with RNA from biopsies of "no cancer" control subjects all of whose biopsies show no cancer, no HGPIN, no atypia and no notable inflammatory changes.

In our first set of Affymetrix gene expression studies we are utilizing samples from 20 study subjects: 5 AA and 5 EA with high grade prostate cancer and 5 AA and 5 EA "no cancer" controls. . As with most gene profiling techniques, the HTA 2.0 array performs best with high quality RNA. As shown in our QC studies summarized in Figure 9, we routinely prepare RNA from biopsy tissue prints with RINs of over 7 (consistent with high RNA quality) and the total RNA per prostate biopsy print is approximately 200 ng. It should be noted that we have sufficient RNA remaining from each biopsy core to perform qrtPCR confirmatory studies of the Affymetrix array "hits".

Our biopsy RNA profiling studies are designed both to discover individual biomarkers associated with high grade prostate cancer in AA and EA patients and to identify molecular subgroups of prostate cancer that may be more prevalent in men of African or European ancestry. It should be noted that the Affymetrix HTA 2.0 array is well suited for this type of analysis; it is currently the most comprehensive array for interrogating human transcripts for expression profiling and includes both coding and long non-coding RNA transcripts. In addition to gene-level detection, the HTA 2.0 provides the necessary coverage and accuracy required to detect all known human transcript isoforms produced from a gene.

We are in the early stages of our HTA 2.0 array studies, and we're exploring different approaches to differential gene expression analysis. The recent publication by Gorlov et al (2014) has provided some particularly helpful guidance for this project. This bioinformatics group notes that although a typical approach to analyzing tumor gene expression is to compare cancer to adjacent uninvolved tissue, an analysis of inter-individual tumor-to-tumor variation in gene expression is often a more efficient way to identify genes that are over or under expressed in a molecular subgroup. One important advantage to this type of analysis is that it is not confounded by tumor associated changes in adjacent normal-looking tissue (cancer "field effects"). In the biopsies from some of our study subjects with extensive prostate cancer, there are no histologically benign cores and the approach of Gorlov et al provides a useful alternative analytical approach.

An example comparing the two approaches to differential gene expression analysis in our prostate biopsy samples is shown in Figure 10. Our pairwise analysis of tumor-to-tumor variation in biopsies from AA and EA patients with high grade prostate cancer has identified several robustly overexpressed "outlier" genes of interest. These **include fatty acid binding protein 5 (FABP5)**, which has previously been identified as an "outlier" in gene profiling studies and defines a PrCa molecular subgroup with a prevalence of 30-40% (Alshalalfa et al 2012). FABP5 overexpression has been implicated in a more aggressive prostate cancer phenotype (lymph node metastasis) (Pang et al 2010). Of particular interest is an association between FABP5 overexpression and enhanced tumor angiogenesis in PrCa xenograft mouse models (Adamson 2003). Prostate cancer induced changes in blood flow and tissue permeability can be imaged non-invasively by MRI, and new technologies that allow fusion of MRI images with the ultrasound used to guide prostate biopsy are moving into the clinic. With the addition of Drs Nix and Rais-Bahrami to our study team, we are planning pilot studies to determine if prostate cancers that overexpress FABP5 represent an aggressive subtype that can be differentiated by prostate MRI.

Studies Related Studies to Support This Grant:

We continue to work in a very successful collaboration with Dr. Clayton Yates at Tuskegee University focusing on racial differences in microRNAs in prostate cancer. Our laboratories continue to work with the laboratory of Dr. Yates in characterizing racial differences in microRNAs of PrCas. From September 2013 to August 2014, 22 paired samples (22 PrCA and 22 matching uninvolved tissues) from 8 AAs and 12 similarly paired samples of PrCa and matching uninvolved prostate from EAs were macrodissected and total RNA (mRNA and microRNA) was extracted from the macrodissected tissue. The RNA was provided to Dr. Yates' laboratory for confirmation of the prior identification of miRs which are expressed differentially in PrCa. Previously, 11 miRs were found to be expressed differentially between PrCa and uninvolved prostate glands at statistically significant p values.

Analysis of the new tissues for microRNAs will be used to confirm the prior results including the results that miR-152 is correlated with increased metastasis and biochemical recurrence, probably via downregulation of DNA methyltransferase (Theodore et al 2014).

Future Directions:

The identification by our Affymetrix studies that the expression of fatty acid binding protein 5 (FABP-5) at the mRNA level may be a marker for an aggressive subset of PrCas is an important observation; FABP-5 has been reported to be increased in cell lines of PrCa as well as PrCa tissues and has been hypothesized to be a tumor suppressor gene (Das et al 2001); however, this and related observations were not pursued and we will verify this observation at the protein level. Because increased levels in plasma of FABP-5 as well as FABP-4 are biomarkers of metabolic syndrome (Bagheri et al 2010), a validated ELISA assay is available for FABP-5 (Biovendor Laboratory Medicine). We will use this ELISA assay to compare plasma levels of FABP-5 from patients with PrCa versus without PrCa and in patients with PrCa, the levels of FABP-5 in plasma for different Gleason scores of PrCa.

As part of the study of FABP-5, immunohistochemistry will be performed on prostates with PrCa and prostates without PrCa (radical cystectomy specimens). The intensity of immunostaining for FABP-5 will be correlated with the Gleason score to characterize more specifically the subsets of PrCa which expresses FABP-5. The cases with varying staining will be analyzed by RT-Q-PCR to verify the mRNA-protein association.

Although we were initially confused about our results on HE4 and other down regulated proteins in patients with PrCa compared to those without PrCa, we have now accepted that low level mRNA of the WFDC2 gene and the decreased matching HE4 protein may be molecular markers of PrCa. Thus, in the next 12 months, we will verify the HE4 results using uniquely designed multiplex assays. These assays will include biomarkers which our preliminary data indicated are both increased and decreased. Paired samples, PrCa and controls, will be matched in analysis based on sample storage times (See Challenges and Problems).

Early in the next funding period, the pilot mass spectrometry study will be analyzed and its results will be completed and correlated with the results from other levels of analysis (Luminex, Affymetrix, RT-Q-PCR assays). Based on these discovery studies, a list of molecules of interest in aggressive prostate cancers will be developed and proteins will be extracted from the nitrocellulose blots to confirm the results from paraffin tissues.

We will continue to work with Dr. Clayton Yates in the analysis of microRNAs in AAs versus EAs. The initial microRNA differentially expressed in PrCa will be continued in additional macrodissected cases. As with microRNA 152 (See References – Theodore et al 2014), the importance of each microRNA in PrCa will be confirmed and racial differences will be evaluated. Also, additional tissues will be macrodissected to separate PrCa from uninvolved prostate glands from radical prostatectomies of the prostate. Total RNA will be extracted and provided to Dr. Yates' laboratory and unstained sections for extraction of proteins will be provided to Dr. Mobley for analysis by mass spectrometry. As in prior cases, AA and EA cases will be matched to detect racial differences. In addition, unstained sections will be provided to Dr. Gaston's laboratory for analysis by RT-PCR analysis for racial admixture studies.

Candidate biomarkers that arise from either the RNA or protein discovery platforms are ranked based on the strength of association with Gleason grade, strength of association with racial ancestry and evidence of likely biological relevance (either from published studies or pathway analysis). We evaluate all top ranked marker candidates in an independent series of samples using qrtPCR, immunohistochemistry or other appropriate methods. For the set of markers that are confirmed in an independent series of samples, we will focus our confirmatory studies on the "hits" that appear to define prostate cancer subgroups that are sufficiently prevalent to be useful clinical markers. For our Affymetrix HTA 2.0 GeneChip studies, our primary focus will be on defining RNA expression patterns that correlate Gleason grade and racial ancestry, including a detailed comparison of gene expression profiles in cancers with a similar histology from AA and EA patients.

For these studies we are working closely with Dr. Towia Liebermann, who is the director of the Harvard Cancer Center Genomics laboratory where we perform our Affymetix GeneChip analysis. Dr. Liebermann is a well-recognized cancer research scientist and an expert in gene expression analysis. Our expression studies include a systems biology analyses that integrates divergent data into a comprehensive analysis of key pathophysiological pathways and analyses that compare the prostate cancer GeneChip data generated by this project with other publically available prostate cancer gene expression datasets to further characterize potentially important subgroups. In addition, our data analysis for the

Affymetrix HTA 2.0 array gene discovery studies includes a comparison of each PrCa RNA profile with a series of baseline reference RNA samples from "no cancer" prostate tissues to help control for confounding field effects in benign tissue adjacent to cancer. We anticipate that analysis of gene expression in "no cancer" prostate tissues from AA and EA men who are free of prostate cancer on biopsy may help identify racial differences that are associated with cancer risk.

In the next reporting period, we will complete several manuscripts focusing on the results of this project. This includes a manuscript on epigenetic regulation of GSTp1, APC and RASSAF in prostate cancer based on NC blots, a manuscript on HE4 (WEFC2) and HE4 isoforms in prostate cancer, and a manuscript of fatty acid binding protein-5. Also, we will complete a manuscript on the use of NC blots in the study of racial differences in prostate cancer.

KEY RESEARCH ACCOMPLLISHMENTS

- We have utilized the Affymetrix gene array to identify a candidate biomarker, fatty acid binding protein-5, which, based on the literature, is associated with the aggressiveness of tumors in general and prostate cancer specifically. The differential expression of this biomarker has been confirmed in a separate set of PrCas using RT-Q-PCR. We will confirm these associations also at the protein level.
- We have concluded the HE4 protein and its gene, WFDC2, are a potential pair of biomarkers that are characteristic of prostate cancer.
- We have successfully completed the contract with Urology Centers of Alabama to obtain nitrocellulose bots on 60 African American men biopsied for prostate cancer. We have demonstrated that at UAB we can use magnetic resonance imaging combined with ultrasound imaging (MRI/US) to identify prostate biopsy sites and that nitrocellulose blots can be obtained from biopsies during MRI/US procedures.
- We have successfully macrodissected 20 radical prostatectomy cases (12 EA and 8 AA). PrCa was separated successfully from uninvolved prostate glands. Sections were provided for discovery studies using mass spectrometry (MS). Initial results were obtained from 5 AA tissue pairs (PrCa and uninvolved glands) and 4 EA pairs. Initial protein from the remaining 11 cases was insufficient for analysis by MS and the remaining 8 EA and 3 AAs have been recut and additional tissues provided for analysis by MS. Also, microRNA was extracted and provided from these cases to the laboratory of Dr. Clayton Yates for confirmation and expression of the previously published results as to microRNA in prostate cancer (Theodore et al 2014). In addition, tissues from these same cases were provided to Dr. Gaston for study of fatty acid binding protein-5 and for analysis of racial admixtures.

REPORTABLE OUTCOMES

- The 60 cases of PrCa from AAs have been collected at UCA completing their contract requirements. Because all required cases of PrCa have been collected at UCA, the IRB for UCA has entered the data analysis category and no additional patients are being accrued at UCA.
- A preliminary study of racial differences in PrCa at the microRNA level has been published (Theodore et al 2014). Additional RNA on matching PrCa and uninvolved prostate from an additional 12 EA and 8 AA patients has been provided to Dr. C. Yates to confirm the initial observations and to expand the analysis of additional microRNAs identified in the preliminary study.
- Several review manuscripts associated with this grant are published and/or in press (listed in body and included in appendix).
- In 2014, all IRBs have been renewed at UAB and UCA. TU work has been classified as exempt.

CHALLENGES AND PROBLEMS:

Identifying biomarkers of prostate cancer that are associated with aggressive subtypes has been a definite challenge due to the numbers of prostate cancer that behave indolently, slowly progress, that may not be identified on initial biopsy, as well as the observation that many of the more aggressive prostate cancers in EAs tend to develop in an older population, and hence, may not be diagnosed until the tumors are late stage. Such cases cause problems in that cryptic PrCas may be in the control group. Thus, there may be an unrecognized overlap between PrCa and control groups. Also, the samples to be analyzed may degenerate on storage after one or two years and this may lead to bias in studies. These problems are being addressed in our future studies.

CONCLUSION

In this reporting period, we have identified using the Affymetrix gene array of mRNA extracted from NC blots that fatty acid binding protein-5 (FABP5) is differentially expressed at the mRNA level in a subgroup of prostate cancers and confirmed this observation by analysis with RT-Q-PCR using a separate set of cases of PrCa. These results are important in that, in the literature, FABP5 has been associated with aggressive features of PrCa. The original descriptions of FABP5 were not confirmed nor expended. However, we consider that FABP5 represents a biomarker which should be further studied and clinically utilized. Also, the approach used to identify and to verify FABP5 as a biomarker will be used with the other Affymetrix data to identify additional biomarkers of PrCa aggressiveness. Similarly, we consider epigenetic control of uninvolved prostate tissue by PrCa to be important in detecting PrCa. Our observations that HE4 may be an epigenetically downregulated molecule will be explored further. Of special interest is differential phenotypic expression of HE4 in serum. We, together with Dr. Clayton Yates, will confirm our reported observations of microRNA expression in PrCa and expand these observations by determining the biology in PrCa of the microRNAs identified to be differentially expressed in PrCa. Thus, in this reporting period, we have begun to identify successfully biomarkers that may be used clinically to identify aggressive subtypes of prostate cancer as well as to detect cryptic foci of prostate cancer that may be missed based on routine approaches to biopsy.

REFERENCES

Alshalalfa M, Bismar TA, Alhajj R. Detecting cancer outlier genes with potential rearrangement using gene expression data and biological networks. Adv Bioinformatics. 2012; 2012:373506. PubMed PMID: 22811706; PubMed Central PMCID: PMC3394389.

Adamson J, Morgan EA, Beesley C, Mei Y, Foster CS, Fujii H, Rudland PS, Smith PH, Ke Y. High-level expression of cutaneous fatty acid-binding protein in prostatic carcinomas and its effect on tumorigenicity. Oncogene. 2003;22(18):2739-49. PubMed PMID: 12743598.

Bagheri R, Qasim AN, Mehta NN, Terembula K, Kapoor S, Braunstein S, Schutta M, Igbal N, Lehrke M, Reilly MP. Relation of plasma fatty acid binding proteins 4 and 5 with the metabolic syndrome, inflammation and coronary calcium in patients with type-2 diabetes mellitus. Am J Cardiol 2010;106(8):1118-23.

Das R, Hammamieh R, Neill R, Melhem M, Jett M. Expression pattern of fatty acid-binding proteins in human normal and cancer prostate cells and tissues. Clin Cancer Res 2001;7(6):1706-15.

Drapkin R, von Horsten HH, Lin Y, Mok SC, Crum CP, Welch WR, Hecht JL. Human epididymis protein 4 (HE4) is a secreted glycoprotein that is overexpressed by serous and endometrioid ovarian carcinomas. Cancer Res 2005;65(6):2162-9.

Gorlov IP, Yang JY, Byun J, Logothetis C, Gorlova OY, Do KA, Amos C. How to get the most from microarray data: advice from reverse genomics. BMC Genomics. 2014;15:223.

Grizzle WE, Srivastava S, Manne U. Translational pathology of neoplasia. Cancer Biomark 2011;9(1-6):7-20. PMCID:PMC3445029.

Kim JH, Dhanasekaran SM, Presner JR, Cao X, Robinson D, Kalyana-Sundaram S, Huang C, Shankar S, Jing X, Iyer M, Hu M, Sam L, Grasso C, Maher CA, Palanisamy N, Mehra R, Kominsky HD, Siddiqui J, Yu J, Qin ZS, Chinnaiyan AM. Deep sequencing reveals distinct patters of DNA methylation in prostate cancer. Genome Res 2011;21(7):1028-41.

McNally LR, Manne U, **Grizzle WE**. Post-transcriptional processing of genetic information and its relation to cancer. Biotech Histochem 2013; 88(7):365-72. PMCID:PMC4091847.

Pang J, Liu WP, Liu XP, Li LY, Fang YQ, Sun QP, Liu SJ, Li MT, Su ZL, Gao X. Profiling protein markers associated with lymph node metastasis in prostate cancer by DIGE-based proteomics analysis. J Proteome Res. 2010;9(1):216-26. PubMed PMID: 19894759.

Potter DM, Butterfield LH, Divito SJ, Sander CA, Kirkwood JM. Pitfalls in retrospective analyses of biomarkers: A case study with metastatic melanoma patients. J Immunol Methods 2012;376(1-2):108-112.

Theodore SC, Davis M, Zhou F, Wang H, Chen D, Rhim J, Dean-Colomb W, Turner T, Ji W, Zeng G, **Grizzle W**, Yates C. MicroRNA profiling of novel African American and Caucasian prostate cancer cell lines reveals a reciprocal regulatory relationship of miR-152 and DNA methyltranferase-1. Oncotarget Advance Publications 2014; 5(11):3512-25. PMCID:PMC4116499.

SUPPORTING DATA

Table 1: Subjects Enrolled in Prostate Biopsy Tissue Print Study as of August 31, 2014

All Subjects	All races		AA		EA	
	N	% of group	N	% of group	N	% of group
All Subjects	**117**	100%	**83**	100%	**34**	100%
No cancer in any core*	**60**	51%	**44**	53%	**16**	47%
High Grade PrCa	**32**	27%	**22**	27%	**10**	29%
Low Grade PrCa	**25**	21%	**17**	20%	**8**	24%

* May have HGPIN or other potentially premalignant findings

No Cancer Subjects	All races		AA		EA	
	N	% of group	N	% of group	N	% of group
No cancer in any core*	60	100%	44	100%	16	100%
No Ca, HGPIN, suspicious	47	78%	37	84%	10	62%
HGPIN, suspicious	13	22%	7	16%	6	38%

* May have HGPIN or other potentially premalignant findings

Low Grade PrCa Subjects	All races		AA		EA	
	N	% of group	N	% of group	N	% of group
Low Grade PrCa	25	100%	17	100%	8	100%
AS Candidate**	14	56%	13	76%	1	12%
Not an AS candidate**	11	44%	4	24%	7	88%

**UCSF Criteria for AS

High Grade PrCa Subjects	All races		AA		EA	
	N	% of group	N	% of group	N	% of group
High Grade PrCa	32	100%	22	100%	10	100%
Highest GS 3+4	20	62%	16	73%	4	40%
Highest GS 4+3 or more	12	38%	6	27%	6	60%

Table 2:

Pre Biopsy Serum PSA All Subjects			
PSA (ng/ml)	**All races**	**AA**	**EA**
Mean	31.2	41.1	7.1
SD	210.0	249.1	7.4
Median	5.4	5.4	4.6
SE	19.4	27.3	1.3
Lowest PSA	0.7	0.7	1.4
Highest PSA	2195.0	2195.0	42.0

Pre Biopsy Serum PSA minus 2 outliers (outliers: 2195 and 634 ng/ml)			
PSA (ng/ml)	**All races**	**AA**	**EA**
Mean	7.2	7.2	7.1
SD	6.7	6.5	7.4
Median	5.4	5.4	4.6
SE	0.6	0.7	1.3
Lowest PSA	0.7	0.7	1.4
Highest PSA	42.0	40.0	42.0

APC ratios

Data summary

Histo-Benign	N	Mean	SD	Median	SE	Min	Max
Group 1	240	14.4	29.9	2.5	1.9	0.0	200.6
Group 2	452	44.2	85.4	9.0	4.0	0.0	638.1
Group 3	289	78.8	198.7	22.5	11.7	0.0	2741.5

Dunn's Multiple Comparisons Test

Comparison		Mean Rank Difference	P Value	Significance
Group 1 Histo Bn	Group 2 Histo Bn	-141.8	<0.001	***
Group 1 Histo Bn	Group 3 Histo Bn	-257.3	<0.001	***
Group 2 Histo Bn	Group 3 Histo Bn	-11548.0	<0.001	***

GSTPi ratios

Data summary

Histo-Benign	N	Mean	SD	Median	SE	Min	Max
Group 1	240	0.9	4.1	0.0	0.3	0.0	46.1
Group 2	451	3.4	12.9	0.0	0.6	0.0	165.3
Group 3	288	11.6	55.3	0.0	3.2	0.0	734.3

Dunn's Multiple Comparisons Test

Comparison		Mean Rank Difference	P Value	Significance
Group 1 Histo Bn	Group 2 Histo Bn	-109.2	<0.001	***
Group 1 Histo Bn	Group 3 Histo Bn	-187.8	<0.001	***
Group 2 Histo Bn	Group 3 Histo Bn	-78.5	<0.001	***

RASSF ratios

Data summary

Cancer Cores	N	Mean	SD	Median	SE	Min	Max
Group 1	240	41.0	79.5	8.6	5.1	0.0	479.9
Group 2	452	98.0	182.9	24.8	8.6	0.0	1573.4
Group 3	289	124.0	261.0	32.7	15.3	0.0	2505.4

Dunn's Multiple Comparisons Test

Comparison		Mean Rank Difference	P Value	Significance
Group 1 Histo Bn	Group 2 Histo Bn	-115.4	<0.001	***
Group 1 Histo Bn	Group 3 Histo Bn	-148.0	<0.001	***
Group 2 Histo Bn	Group 3 Histo Bn	-32.62	P> 0.05	ns

Table 3. APC, GSTPi and RASSF1 Methylation Ratios in the Histologically Benign Cores

APC ratios

Data summary

Cancer Cores	N	Mean	SD	Median	SE	Min	Max
Group 2 GIs 6	64	114.5	149.8	59.8	18.7	0	603.8
Group 3 GIs 6	37	221.4	258.9	116.7	42.6	5.6	1047.7
Group 3 GIs 3+4	41	191.4	175.7	136.6	27.4	3.4	860.2
Group 3 GIs 4+3+	16	151.7	174.6	78.0	43.6	17.8	674.2

Dunn's Multiple Comparisons Test

Comparison		Mean Rank Difference	P Value	Significance
Group 2 GIs 6	Group 3 GIs 6	-25.713	< 0.05	*
Group 2 GIs 6	Group 3 GIs 3+4	-30.722	< 0.01	**
Group 2 GIs 6	Group 3 GIs 4+3+	-19.117	>0.5	ns
Group 3 GIs 6	Group 3 GIs 3+4	-5.009	>0.5	ns
Group 3 GIs 6	Group 3 GIs 4+3+	6.596	>0.5	ns
Group 3 GIs 3+4	Group 3 GIs 4+3+	11.6	>0.5	ns

GSTPi ratios

Data summary

Cancer Cores	N	Mean	SD	Median	SE	Min	Max
Group 2 GIs 6	64	25.1	50.4	6.1	6.3	0	283.8
Group 3 GIs 6	37	80.0	98.9	31.0	16.3	0	333.1
Group 3 GIs 3+4	41	88.4	124.2	26.1	19.4	0	415.0
Group 3 GIs 4+3+	16	92.9	129.2	23.5	32.3	0	437.9

Dunn's Multiple Comparisons Test

Comparison		Mean Rank Difference	P Value	Significance
Group 2 GIs 6	Group 3 GIs 6	-33.439	< 0.01	**
Group 2 GIs 6	Group 3 GIs 3+4	-28.48	< 0.05	*
Group 2 GIs 6	Group 3 GIs 4+3+	-28.445	>0.5	ns
Group 3 GIs 6	Group 3 GIs 3+4	4.960	>0.5	ns
Group 3 GIs 6	Group 3 GIs 4+3+	4.994	>0.5	ns
Group 3 GIs 3+4	Group 3 GIs 4+3+	0.034	>0.5	ns

RASSF ratios

Data summary

Cancer Cores	N	Mean	SD	Median	SE	Min	Max
Group 2 GIs 6	64	270.1	358.4	124.2	44.8	0	1603.2
Group 3 GIs 6	37	419.1	390.6	265.6	64.2	0.4	1446.0
Group 3 GIs 3+4	41	515.9	552.3	282.7	86.2	0	2302.6
Group 3 GIs 4+3+	16	686.4	983.08	292.7	245.77	0	3198.8

Dunn's Multiple Comparisons Test

Comparison		Mean Rank Difference	P Value	Significance
Group 2 GIs 6	Group 3 GIs 6	-21.75	>0.5	ns
Group 2 GIs 6	Group 3 GIs 3+4	-27.24	< 0.05	*
Group 2 GIs 6	Group 3 GIs 4+3+	-26.33	>0.5	ns
Group 3 GIs 6	Group 3 GIs 3+4	-5.50	>0.5	ns
Group 3 GIs 6	Group 3 GIs 4+3+	-4.58	>0.5	ns
Group 3 GIs 3+4	Group 3 GIs 4+3+	0.91	>0.5	ns

Table 4: APC, GSTPi and RASSF1 Methylation Ratios in the Cancer Cores

Figure 1: Field Effect Study Overview

Primary Question:

Is the Epigenetic Hypermethylation of APC, GSTPi and RASSF1 Sensitive to the Gleason Grade of an Adjacent Prostate Cancer?

Study Groups:

Group 1: 20 prostate biopsy patients with no prostate cancer, HGPIN or suspicious histology
Group 2: 46 prostate biopsy patients diagnosed with minimal Gleason 3+3 prostate cancer
Group 3: 36 prostate biopsy patients diagnosed with at least one core of Gleason 7 (3+4 or 4+3) prostate cancer

Total: 102 study subjects with 12 biopsy cores for each subject
1224 total biopsy cores

Biomarker Assay:

Multiplex methylation sensitive PCR for APC, GSTPi and RASSF1 promoter hypermethylation

Major findings:

The level of hypermethylation in the histologically benign biopsy cores is positively correlated with the level of hypermethylation in the cancer cores.

The level of hypermethylation in the benign biopsy cores increases significantly with the Gleason grade in the cancer cores

The level of hypermethylation in a Gleason 6 cancer is significantly higher in Group 2 (Gleason 6 only) than in Group 3 (which has a high grade focus elsewhere in the gland).

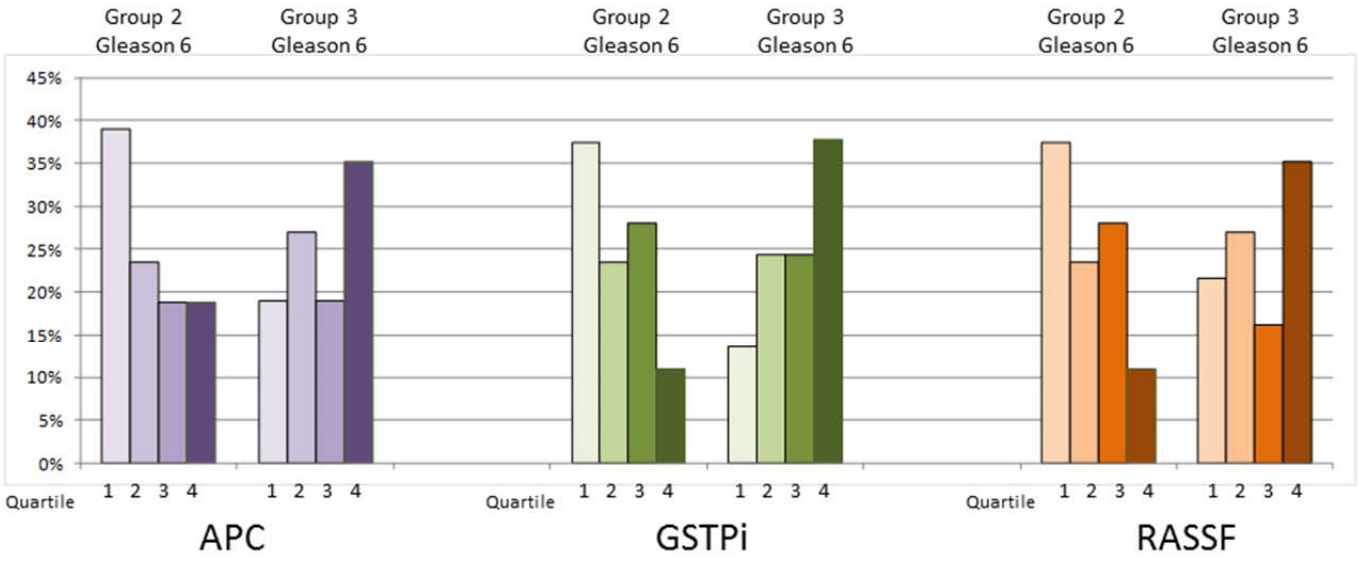

Figure 2: Hypermethylation marker profiles of Gleason 3+3 Biopsy Cores in Group 2 vs Gleason 3+3 Biopsy Cores in Group 3 . The data is plotted as quartiles, with darker shades of each color corresponding to higher levels of hypermethylation. For all three markers, the Gleason 3+3 cores from group 3 are more highly methylated than the Gleason 3+3 cores from group 2

Group 2: subjects whose cancer cores show only Gleason 3+3

Group 3: subjects who have one or more Gleason 7+ cores

Figure 3 – Due to the large size of Figure 3 and the email limitations, Figure 3 will be uploaded thru UAB's dropbox.

Figure 4 – Due to the large size of Figure 4 and the email limitations, Figure 4 will be uploaded thru UAB's dropbox.

Figure 5:

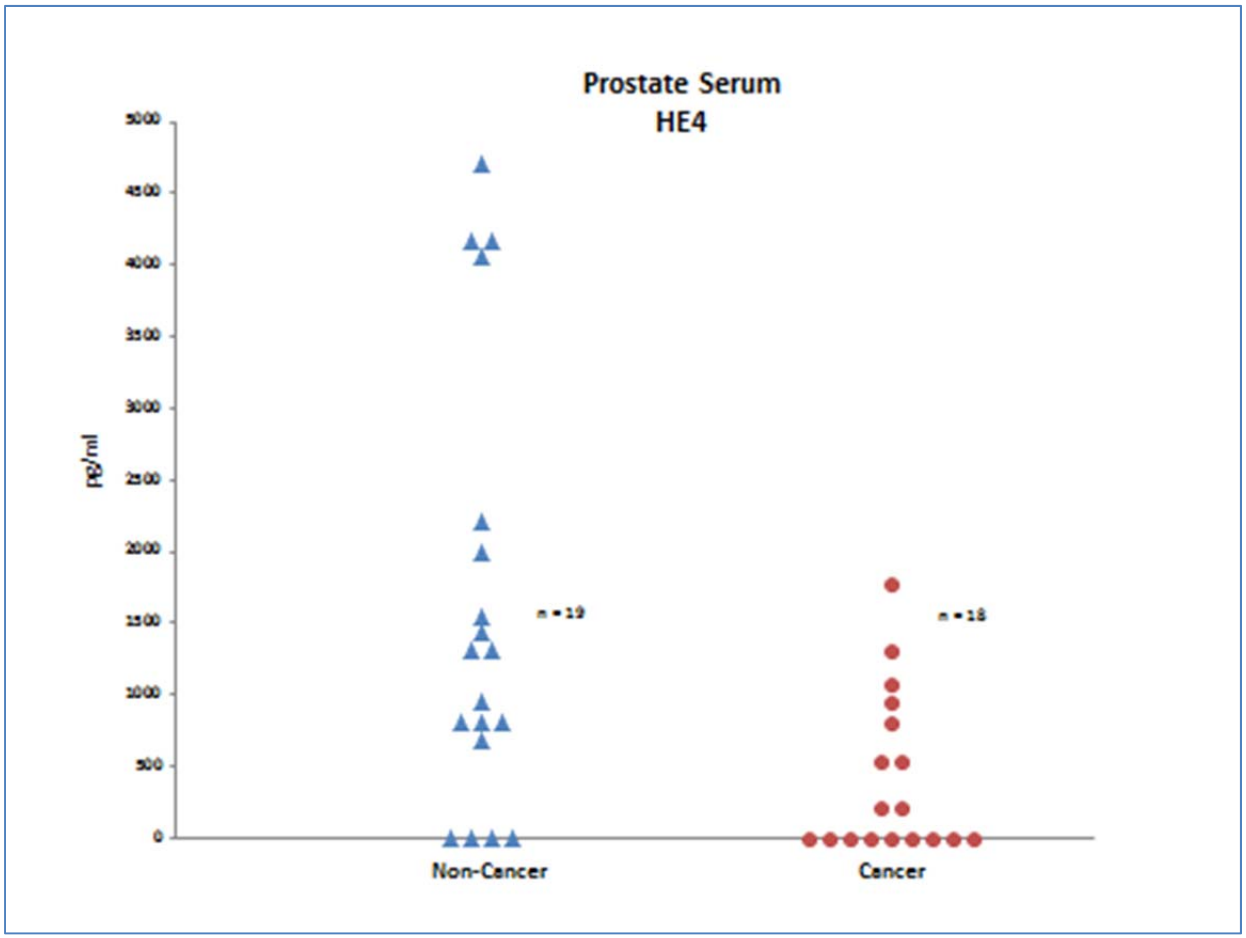

Figure 6 – Due to the large size of Figure 6 and the email limitations, Figure 6 will be uploaded thru UAB's dropbox.

Figure 7 – Due to the large size of Figure 7 and the email limitations, Figure 7 will be uploaded thru UAB's dropbox.

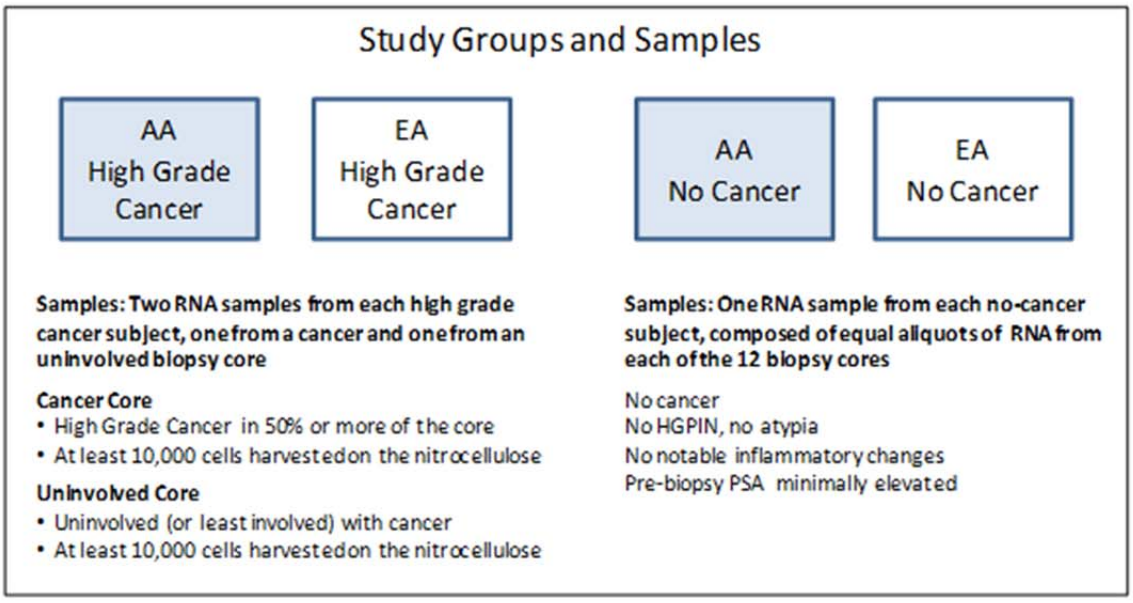

Design of Affymetrix Array 2.0 mRNA profiling study

Note that in some cases there is no biopsy core that is uninvolved with cancer. In such instances, we compare the most and least involved cores.

Sample ID	Status	RIN number	RNA conc in sample (ng/µl)	Total RNA in sample (ng)
1012-A	Tumor 1	7.3	8.06	403
1012-B	Benign 1	7.2	6.11	306
1016-A	Tumor 1	7.9	23.46	1,173
1016-B	Tumor 2	6.0	9.95	497
1014-A	Tumor 1	8.6	35.14	1,757
1014-B	Benign 1	7.1	10.11	505
1028-A	Tumor 1	≈ 7	28.68	1,434
1028-B	Benign 1	7.7	33.99	1,699
2016-A	Tumor 1	3.8	6.13	307
2016-B	Benign 1	7.0	4.89	244
1007-A	Tumor 1	≈ 7	10.46	523
1007-B	Tumor 2	9.6	19.25	963
1023-A	Tumor 1	8.3	14.99	750
1023-B	Tumor 2	8.3	26.02	1,301
2035-C	Entirely Benign	8.5	9.56	478
2023-C	Entirely Benign	7.6	19.49	975
471-C	Entirely Benign	8.7	33.87	1,694
451-C	Entirely Benign	7.9	136.35	6,817

Figure 8 Agilent Bioanalyzer analysis of biopsy tissue print RNA

Subject P1007
African American
Age 60-65
Pre-biopsy PSA >1000

	Left	Right
Base	GI 4+3 90% PNI	GI 4+5 90%
Middle	GI 4+3 90% PNI	GI 4+3 70%
Apex	GI 4+3 70% PNI	GI 4+5 60%

Subject P1023
African American
Age 60-65
Pre-biopsy PSA 20

	Left Lateral	Left Medial	Right Medial	Right Lateral
Base	GI 3+4 70% PNI	GI 3+5 80% PNI	GI 3+3 5%	GI 3+4 80%
Middle	GI 3+4 80% PNI	GI 3+4 90% PNI	GI 3+4 40%	GI 3+3 20%
Apex	GI 3+4 80% PNI	GI 3+4 95% PNI	GI 3+4 80% PNI	GI 3+4 5%

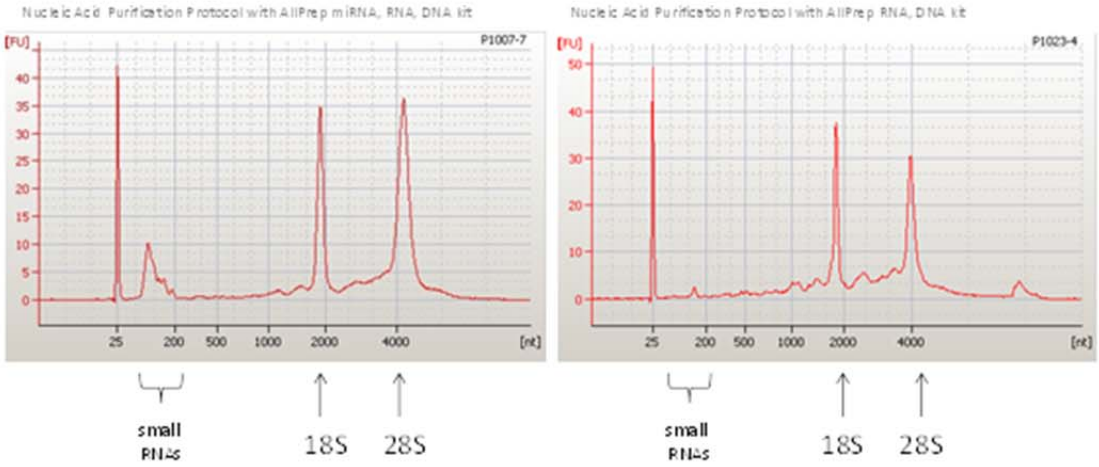

Sample ID	Prosate Biopsy Histology	Total Cells on Biopsy Print (Quantifiler)	RNA Concentration (ng/µl)	Total RNA (ng)	RIN Number
P1007-7	90% Gleason 4+5	214,929	19.3	962.6	9.6
P1023-4	80% Gleason 3+5	161,322	15.0	749.6	8.3

Figure 9. Examples of Bioanalyzer Analysis of Biopsy Tissue Print RNA Quality

Examples of biopsy tissue print RNA obtained from biopsy tissue prints from biopsies with a high % of high grade prostate cancer are shown above. Note that sample P1007-7 was prepared using a protocol that recovers microRNAs while sample P1023-4 was prepared using our standard AllPrep RNA DNA protocol. The difference in recovery of microRNAs can be visualized in the Bioanalyzer tracing (in the zone marked "small RNAs")

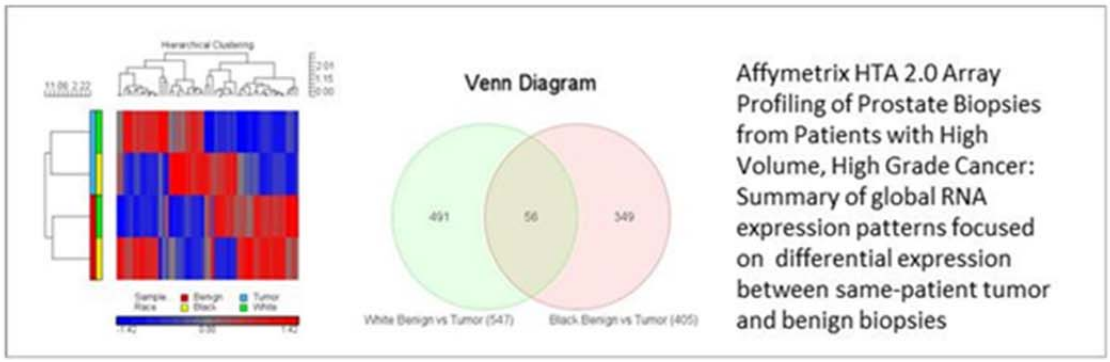

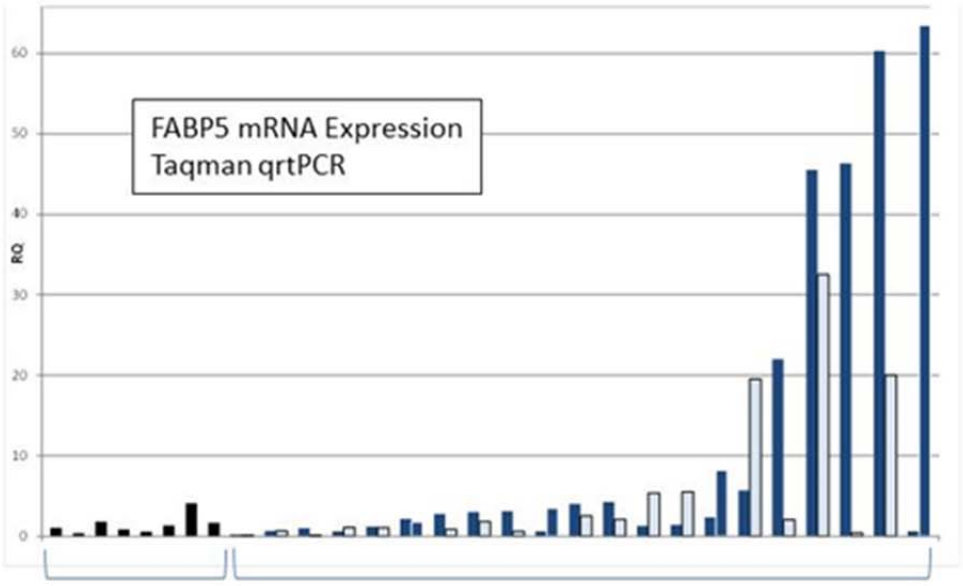

Expression analysis focused on Tumor-to-Tumor comparisons (Orlov et al 2014) is a method for identification of prostate cancer subgroups that minimizes confounding field effects in tumor adjacent benign tissue. This has proven to be an efficient strategy for identifying candidate genes that are confirmed by qrtPCR in independent samples

Figure 10. Tumor-to-Adjacent Benign and Tumor-to-Tumor Comparisons of Gene Expression Profiles for Prostate Cancer Biomarker Discovery.

APPENDICES

Cumulative Publications Resulting from this DOD Grant: (Manuscripts were submitted in a timely fashion with previous reports)

A. Zhang HG, **Grizzle WE**. The effects of exosomes and related vesicles on cancer development, progression and dissemination. *In: Emerging Concepts of Tumor Exosome-Mediated Cell-Cell Communication*, (Eds HG Zhang), Springer Science. 2012;107-129.
B. McNally LR, Manne U, **Grizzle WE**. Post-transcriptional processing of genetic information and its relation to cancer. Biotech Histochem 2013; 88(7):365-72. **(This was in press during the last report. A final version of the published manuscript is included).**
C. Srivastava S., **Grizzle WE**. Biomarkers and the genetics of early neoplastic lesions. Cancer Biomark 2011;(9)(1-6):41-64. NIHMSID:NIHMS402044.
D. **Grizzle WE**, Srivastava S, Manne U. The biology of incipient, pre-invasive or intraepithelial neoplasia. Cancer Biomark 2011;9(1-6):21-39.
E. **Grizzle WE**, Srivastava S, Manne U. Translational pathology of neoplasia. Cancer Biomark 2011;9(1-6):7-20. NIHMSID: NIHMS402047.
F. **Gaston SM,** Guerra AL, Grooteclaes M, Renard, I, Kearney MC, Bigley J and Kearney GP. Gene Methylation Biomarker Analysis of Prostate Biopsies from Men with 1 of 12 Cores Positive for Cancer: Greater Methylation Prevalence and Extent in Gleason 7 than Gleason 6 Cancer. American Urological Association Annual Meeting, Washington DC; May 2011.
G. **Gaston SM**, Kearney GP, **Grizzle WE**. Prostate biopsy tissue print technologies; a practical and innovative approach to overcoming racial disparities in the datasets used for prostate cancer biomarker development. Presented at the AACR Cancer Health Disparities Meeting, Washington, D.C., September 18, 2011.
H. Otali D, He Q, Stockard CR, **Grizzle WE**. Preservation of immunorecognition by transferring cells from 10% neutral buffered formalin to 70% ethanol. Biotech Histochem 2013; 88(3-4):170-80.
I. Jones J, **Grizzle W**, Wang H, Yates C. MicroRNAs that affect prostate cancer: emphasis on prostate cancer in African Americans. Biotech Histochem 2013; 88(7):410-24.
J. **Grizzle WE**, Sexton KC, Bell WC. Human Tissue Biorepository. *In: Molecular Genetic Pathology*, volume 1, 2nd edition. (Eds. L Cheng, D. Zhang, Eble J), Springer Science+Business Media. 2013;483-497.
K. Bledsoe MJ, **Grizzle WE**. Use of Human Tissue in Research: The Current US Regulatory, Policy, and Scientific Landscape. Diagnostic Path 2013;19(9):322-330.
L. Zhang HG, **Grizzle WE**. Exosomes: a novel pathway of local and distant intercellular communication that facilitates the growth and metastasis of neoplastic lesions. Am J Pathol 2014;184(1):28-41.
N. **Gaston SM**, Hayek JE, Otto G, Yen J, Bigley J, Neste LV, Kearney GP. Epigenetic field effect markers are indicative of occult high grade prostate cancer. Presented at the 2013 ASCO Genitourinary Cancers Symposium.
O. **Grizzle WE**. It is primarily the control of transcription and post-transcriptional processing that are critical to the development and progression of sporadic neoplasias. Biotech Histochem 2013; 88(7):361-4.

Publications since last report (**included in Appendix**):

P. Theodore SC, Davis M, Zhou F, Wang H, Chen D, Rhim J, Dean-Colomb W, Turner T, Ji W, Zeng G, **Grizzle W**, Yates C. MicroRNA profiling of novel African American and Caucasian prostate cancer cell lines reveals a reciprocal regulatory relationship of miR-152 and DNA methyltranferase-1. Oncotarget Advance Publications 2014; 5(11):3512-25. PMCID:PMC4116499.
Q. Auer H, Mobley J, Ayers L, Bowen J, Chuaqui R, Johnson L, Livolsi V, Lubenski I, McGarvey D, Monovich L, Moskaluk C, Rumpel C, Sexton K, Washington M, Wiles K, **Grizzle W**, Ramirez N. The effects of frozen tissue storage conditions on the integrity of RNA and protein. Biotech Histochem 2014;89(7):518-528.
R. Van Neste L, Van Criekinge W, Bigley J, **Grizzle WE**, Adams GW, Karney GP, **Gaston SM**. To be presented at the EAU Section of Urological Research (ESUR) meeting in October 9-11, 2014, Glasgow, Scotland.

MicroRNA profiling of novel African American and Caucasian Prostate Cancer cell lines reveals a reciprocal regulatory relationship of *miR-152* and DNA methyltranferase-1

Shaniece C. Theodore[1], Melissa Davis [3], Fu Zhou[1] , Honghe Wang[1], Dongquan Chen[6], Johng Rhim[2] , Windy Dean-Colomb[7], Timothy Turner[1], Weidong Ji [5], Guohua Zeng [5], William Grizzle[4],Clayton Yates[1,4]

[1] Department of Biology and Center for Cancer Research, Tuskegee University, Tuskegee, AL

[2] Center for Prostate Disease Research, Department of Surgery, Uniformed Services University of the Health Sciences, Bethesda, MD

[3] Department of Genetics, University of Georgia, Athens, GA

[4] Department of Pathology, University of Alabama at Birmingham School of Medicine, Birmingham, AL

[5] Department of Urology, Minimally Invasive Surgery Center, The First Affiliated Hospital of Guangzhou Medical College, Guangdong Provincial Key Laboratory of Urology, 1 Kangda Road, Guangzhou 510230, China

[6] Division of Preventive Medicine, University of Alabama at Birmingham School of Medicine, Birmingham, AL

[7] Department of Oncologic Sciences, University of South Alabama Mitchell Cancer Institute, Mobile, AL

Correspondence to: *Clayton Yates,* ***email***: *cyates@mytu.tuskegee.edu*

Keywords: miRNA, DNA methylation, African American, prostate cancer

Received: *April 9, 2014* ***Accepted***: *May 7, 2014* ***Published***: *May 8, 2014*

This is an open-access article distributed under the terms of the Creative Commons Attribution License, which permits unrestricted use, distribution, and reproduction in any medium, provided the original author and source are credited.

ABSTRACT

miRNA expression in African American compared to Caucasian PCa patients has not been widely explored. Herein, we probed the miRNA expression profile of novel AA and CA derived prostate cancer cell lines. We found a unique miRNA signature associated with AA cell lines, independent of tumor status. Evaluation of the most differentially expressed miRNAs showed that miR-132, miR-367b, miR-410, and miR-152 were decreased in more aggressive cells, and this was reversed after treatment of the cells with 5-aza-2'-deoxycytidine. Sequencing of the miR-152 promoter confirmed that it was highly methylated. Ectopic expression of miR-152 resulted in decreased growth, migration, and invasion. Informatics analysis of a large patient cohort showed that decreased miR-152 expression correlated with increased metastasis and a decrease in biochemical recurrence free survival. Analysis of 39 prostate cancer tissues with matched controls (20 AA and 19 CA), showed that 50% of AA patients had statistically significant lower miR-152 expression compared to only 35% of CA patients. Ectopic expression of miR-152 in LNCaP, PC-3, and MDA-PCa-2b cells down-regulated DNA (cytosine-5)-methyltransferase 1 (DNMT1) through direct binding in the DNMT1 3'UTR. There appeared to be a reciprocal regulatory relationship of miR-152/DNMT1 expression, as cells treated with siRNA DNMT1 caused miR-152 to be re-expressed in all cell lines. In summary, these results demonstrate that epigenetic regulation of miR-152/DNMT1 may play an import ant role in multiple events that contribute to the aggressiveness of PCa tumors, with an emphasis on AA PCa patients .

INTRODUCTION

The most commonly diagnosed type of cancer among men in the US is prostate cancer (PCa), which accounts for 29% (241,740) of all new cancer cases. Although the number of new cases of PCa has decreased in recent years, there are still racial and ethnic differences in PCa epidemiology. African-Americans (AAs) have the world's highest incidence of PCa and more than twofold higher mortality rate compared with Caucasian Americans

(CAs) [1]. Overall, AA patients are younger and have higher Gleason scores, PSA levels, and incidence of palpable disease [2]. Various factors have been associated with the more aggressive prostate tumors. For example, differential gene expression in AA patients contributes to aggressive disease [3-7], and epigenetic mechanisms, such as DNA methylation, result in the loss of key regulatory genes [8, 9]. This is particularly evident for AA patients where hypermethylation of genes in normal or pre-malignant areas are thought to predispose to malignancy [10, 11]. However, the underlying mechanism of these acquired methylation patterns is poorly understood.

MicroRNAs (miRNAs) are small RNA molecules consisting of 19–23 nucleotides that regulate various biological processes. More than 60% of protein-coding genes may be targeted by miRNAs [12], mainly through translational repression and degradation of target mRNAs. An expanding body of evidence supports a role for miRNAs in disease progression and the potential for epigenetic mechanisms, such as DNA methylation, to regulate miRNA expression [13, 14]. Recently, DNA methylation of proximal CpG islands in miRNA promoters was described as a method for decreased expression in various cancers, including PCas [15-18]. Although miRNAs are expressed differently in healthy tissues and cancers [19] and in localized and advanced tumors [20], little is known about racial differences in miRNA expression. Identification of unique miRNAs and mRNA-associated targets will begin to clarify the specific events involved in the progression of PCas in AAs.

To address this question, our laboratory has established non-malignant and malignant cell lines derived from AA PCas that replicate many of the clinical features of the original PCas [21, 22]. Thus, utilizing these cell lines and commonly available PCa cell lines, we explored the possibility of race-related differences in miRNA expression. Herein, we report that AA cell lines have a distinct miRNA signature, independent of tumor status. Evaluation of the miRNAs most differentially expressed demonstrated that miR-132, miR-367b, miR-410, and miR-152 were decreased in more aggressive cells and that this expression was reversed after treatment of the cells with 5-aza-2′-deoxycytidine (5-aza-2'd). Bisulfite conversion and sequencing of the promoter showed that miR-152 was highly methylated in LNCaP and PC-3 cells. Ectopic expression of miR-152 resulted in decreased cell proliferation, migration, and invasion. In a panel of 39 PCa tumors with adjacent matched controls (20 AA and 19 CA) , 50 % of AA patients and 35% of CA patients demonstrated statistically significant lower miR-152 expression compared to adjacent controls. Ectopic expression of miR-152 down-regulated DNA(cytosine-5)-methyltransferase 1 (DNMT1) through direct binding in the DNMT1 3'UTR. This appeared to be an inverse relationship, as cells treated with DNMT1 siRNA re-expressed miR-152. Finally, as determined with a large patient cohort, loss of miR-152 was related to poor clinical outcomes including decreased biochemical recurrent free survival.

RESULTS

miRNA Profile of Panel of AA and CA Cell Lines

To determine the miRNA expression pattern in our panel of AA and CA prostate cell lines, the expression of 662 miRNAs was analyzed utilizing Asuragen Affymetrix Gene Chips. To validate the malignant and non-malignant status of this cell line panel, we first preformed hierarchical clustering (Figure 1a) and a PLS plot (Figure 1b), using reported non-malignant and malignant status as the grouping criteria. Both analysis demonstrated distinct expression patterns in the malignant and non-malignant cell lines, with 21 differentially expressed miRNAs between the groups (Supplemental Table 1 ($p<0.00001$). To further determine race related miRNAs, we performed a separate hierarchical clustering analysis on the same data set utilizing racial background as the grouping criteria. Distinct hierarchical clustering of miRNAs was evident between the AA and CA cell lines (Figure 1c), regardless of malignancy status. A PLS plot reflected this pattern, with distinct variations in the racial profiles of the AA and CA cell lines (Figure 1d). In this variation, there were 47 miRNAs differentially expressed by race (Supplemental Table 2). To confirm these 47 miRNAs are race related, we interrogated a microarray dataset that consisted of primary tumor cells isolated from 5 AA and 4 CA patients (Supplemental Table 3). These race related miRNA probes were able to differentiate patients relevant to race using PLS plot test (Supplemental Figure 1).

To if these miRNA's have a relationship to prostate cancer progression, took the most significantly differentially expressed race related miRNA's ($p<0.00001$) (Table 1), and performed qRT-PCR validation within our prostate cancer cell line progression model. Of the 11 miRNAs, we confirmed the 5 most significant by qRT-PCR in non-malignant and selected aggressive malignant cell lines (Supplementary Figure 2). With the exception of miR-363, which did not exhibit a clear expression pattern, miR-132, miR-376b, miR-410 and miR-152 exhibited a decreased expression profile as the metastatic capability of cell lines increased. Thus, we chose these miRNAs for further analysis.

Demethylation Treatment Reverses miRNA Expression of AA-Associated miRNAs.

Previous reports and *in silico* analyses have demonstrated that a majority of the miRNAs we found associated with race contain CpG islands within the

Table 1: Hierarchical clustering of race related miRNAs	
miRNA	(Adjusted) p-value ↑
hsa-miR-363	3.43e-05
hsa-miR-132	0.000354
hsa-miR-376b	0.00188
hsa-miR-410	0.00291
hsa-miR-152	0.00471
hsa-miR-189	0.00498
hsa-miR110	0.00514
hsa-miR-27b	0.00657
hsa-miR-519c	0.0071
hsa-miR-520h	0.00774
hsa-miR-27a	0.00837
**miRNAs separated by race are listed based on p-value	

promoter regions upstream of the start site (Supplemental Figure 3). To determine if hypermethylation is associated with decreased expression of these miRNAs, LNCaP and PC-3 cells were treated with 5 μM 5-aza-2'd alone for three days or in combination with 100 nM TSA for 24 hr. Re-expression of multiple miRNAs was evident in both LNCaP and PC-3 cells after 5-aza-2'd treatment. However, miR-376b and miR-152 showed the most substantial increases in both cell lines (Figure 2).

Since miR-152 contained the greatest percentage of methylated CG sequences and demonstrated the most consistent increases after 5-aza-2'd treatment, we focused on this miRNA. To determine the methylation status of the miR-152 promoter region, we extracted DNA from LNCaP and PC-3 cell lines and preformed sodium bisulfite modification prior to sequencing. To confirm these results, sodium bisulfite-converted DNA was subjected to capillary electrophoresis and analyzed utilizing the online Bisulfite Sequencing DNA Methylation Analysis (BISMA) sequencing program. The results indicated that DNA of both LNCaP and PC-3 cell lines was 100% methylated at 1000 base pairs upstream from the promoter region (Figure 3). Thus, these results suggest that in malignant PCa cell lines, miR-152 is inactivated through hypermethylation.

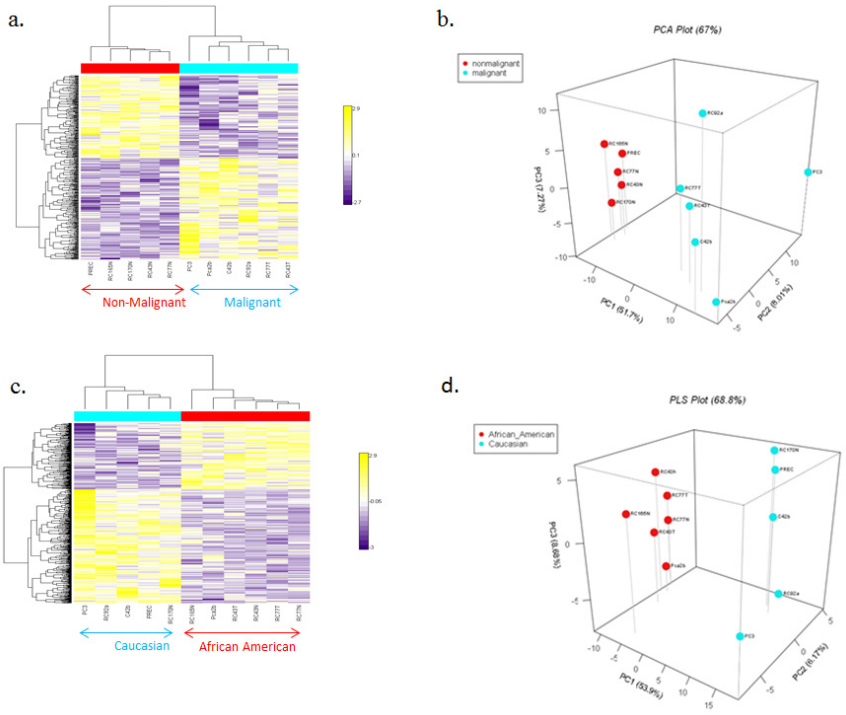

Fig. 1: Heat Map of miRNA microarray. (a) Hierarchical clustering analyses of miRNAs (left) grouped by non-malignant and malignant status: non-malignant cell lines (red block), malignant cell lines (blue block). (b) PLS plot of AA and CA prostate cell lines grouped by malignancy. (c) Hierarchical clustering analyses of miRNAs (left) grouped by race. AA cell lines (red block), CA cell lines (blue block). miRNAs are ordered according to their cluster determined by p-values using the Kruskal-Walis test. (d) PLS plot of AA and CA prostate cell lines grouped by race.

miR-152 Expression Correlates with Clinical and Pathological Variables.

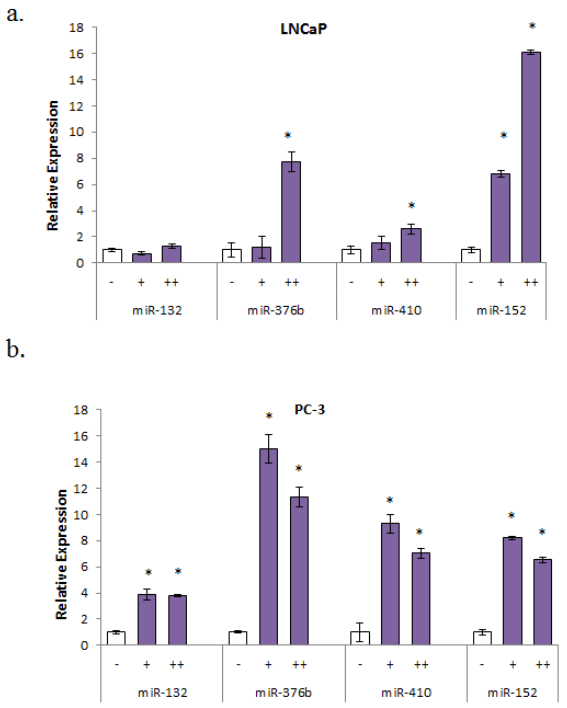

Fig. 2: Multiple miRNA expression pattern after treatment with demethylation agent (a) LNCaP cells were treated with 5 μM 5-aza-2'd for 4 days alone (+) or with 100 nM TSA for 24 hr (++). Results shown are representative of three independent experiments ± s.e.*P<0.05. (b) PC-3 cells were treated with 5 μM 5-aza-2'd for 4 days alone (+) or with 100 nM TSA for 24 hours (++). Results shown are representative of three independent experiments ± s.e. *P<0.05.

The expression of miR-152 in 28 normal cell lines, 97 primary tumors, and 13 metastases was analyzed using the Taylor et al. GSE21032 data set available on the GEO website (http://www.ncbi.nlm.nih.gov/geo/). Primary and metastatic tumors had lower levels of miR-152 relative to normal samples (Figure 4a), which correlated with the higher incidence of metastatic samples, metastatic events, and lymph node invasion (Figures 4b and c). Tumors with low miR-152 levels also had reduced biochemical recurrence-free survival (Figure 4c). Together, this describes a consistent picture of low miR-152 levels associated with PCa metastasis and recurrence.

These results prompted us to determine miR-152 expression in our patient cohort of AAs and CAs, hypothesizing that tumors from AAs would have lower miR-152 than those from CA patients. Patients were selected based on cancers of higher total Gleason score (≥6) and/or pathological stage (pT2), and positive for perineural and/or vascular invasion, as these pathological characteristics correlate positively with tumor aggressiveness and metastasis. AA patients had a lower median age relative to similarly staged CA patients, which was also associated with lower miR-152 levels measured by qRT-PCR (Table 2, p<.001). Analysis of miR-152 expression in individual tumors compared to matching adjacent normal controls showed a statistically significant decrease in miR-152 expression in 50% of the AA patients compared to only 35 % of CA patients (Figure 5a, b Supplemental table 4).

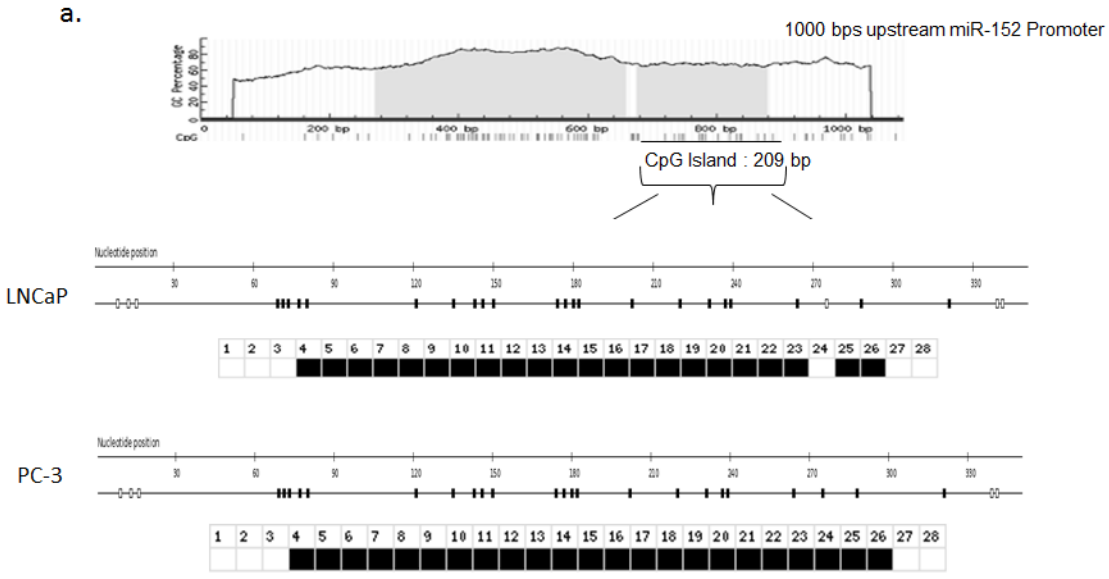

Fig. 3: Bisulfite Sequencing of CpG islands in the miR-152 promoter. (a) Schematic map of the CpG islands in the *miR-152* promoter using UCSC Genome Browser. CpG islands are indicated as vertical lines on map. (b) Bisulfite modification was performed on LNCaP and PC-3 cells, and DNA was sequenced to determine the methylation status of the promoter region. Bisulfite sequencing was analyzed by BDPC software *(see Methods*). Open square; unmethylated CpG; closed circle, methylated CpG.

Table 2: Clinical Characteristics of Paired Primary Tumor Prostate Samples				
Ethnicity		African American	Caucasian	p†
Samples		20 (51.3%)	19 (48.7%)	
Age				
Median		57.5	64	
Mean		57.3	60	
Standard deviation		6.68	7.3	
Min - Max		47-69	48-70	
Initial Clinical Stage				
T1		NA	NA	
T2		16 (80%)	10(52.6%)	
T3		4 (20%)	8 (42.1%)	
NS		NA	1 (5.3 %)	
Gleason Score				
6		8 (40%)	8 (42.1%)	
7		12 (60%)	10 (52.6%)	
8		NA	1 (5.26)	
miR-152 Expression				
Average All Samples ±SD		1.6±	2.6±	p<.001*
†P value with * is deemed significant utilizing F- test . NA- none SD- Standard Deviation				

Restoring miR-152 Expression Decreases Cell Growth.

The clinical relevance of miR-152 in PCa prompted us to determine if loss of expression had a biological or functional role in promoting metastatic tumors. After optimizing the concentration of miR-152 mimics that restored miR-152, miR-152 was transfected into LNCaP, PC-3, and MDA-PCa-2b cells. As determined by MTT assays, ectopic expression of miR-152 inhibited cell proliferation after 3 days, and this continued to Day 6 (Figure 6 a,b,c). Since the inhibition of cell proliferation began at 72 hr, miR-152 transfected cells were next assayed after 72 hr by flow cytometry to determine if there was an effect on cell cycle progression. miR-152 treatment caused cells to accumulate at the G2-M phase (LNCaP NC 22.90% compared to miR-152-transfected cells 30.2%; PC-3 NC 19.9% vs miR-152 transfected cells 29.3%; MDA-PCa-2b NC 33.15 vs miR-152 transfected cells 37.59%) (Figure 6 d, e, f). In addition to reduced cell proliferation, miR-152 transfected LNCaP, PC-3, and MDA-PCa-2b cells demonstrated a decrease in cell migration (Figure 6g) and invasion (Figure 6h).

Previously, miR-152 was demonstrated to target DNMT1 expression in endometrial tumors [23]. Since we observed that numerous miRNAs in our panel were influenced by methylation, and the methyltransferase DNMT1 is a regulator of DNA hypermethylation in various tumor types, we sought to explore the miR-152/DNMT1 relationship in PCas. First, the relative expressions of DNMT1 and miR-152 were examined in our panel of cell lines. As expected, qRT-PCR showed that DNMT1 expression was elevated in the more aggressive cell lines, and this correlated with decreased expression of miR-152 (Figure7a).

DNMT1 expression was then examined in LNCaP, PC-3, MDA-PCa-2b cells transfected with miR-152. Both types of cells showed statistically significant decreases in DNMT1 expression at the RNA and protein levels (Figure 7b). This relationship is possibly direct, as miR-152 has putative binding sites in position 45-54 of the DNMT1 3' UTR. To confirm this, we utilized a previously established DNMT1 3′-UTR luciferase reporter system [24] containing the miR-152-binding sites (DNMT1 wild-

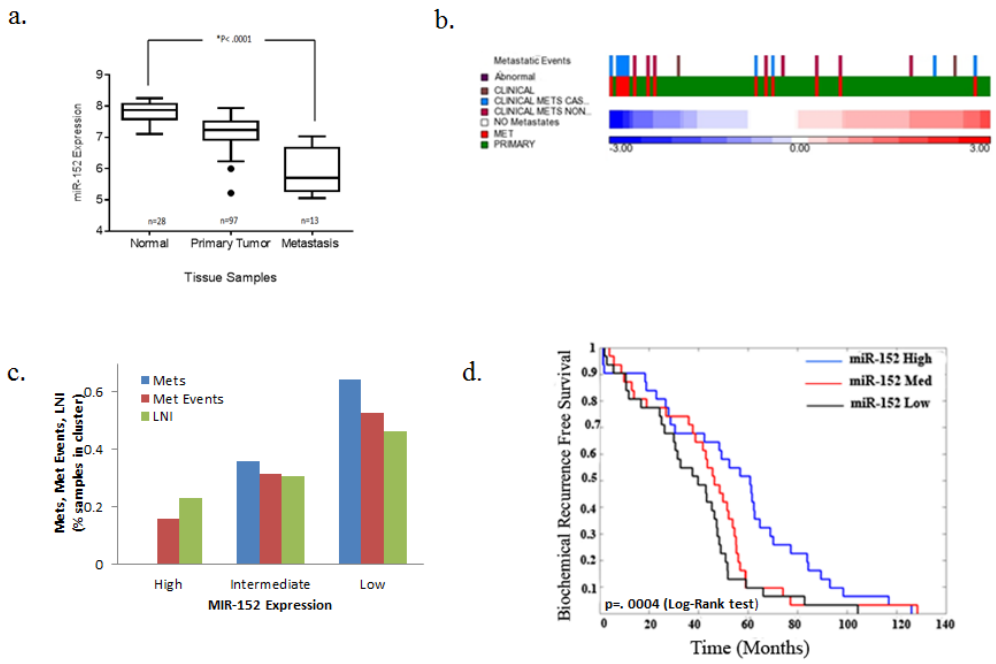

Fig. 4: Low miR-152 expression correlation with PCa metastasis. Taylor et al data set samples were sorted by average miR-152 expression and the mean from two probes was normalized with z-score. (a-d) miR-152 expression correlates with metastases, invasion events, and recurrence-free survival in 138 PCa samples (97 primary tumors and 13 metastases). (a) miR-152 levels decrease monotonically from normal, primary tumor, and metastasis, $P < 0.0001$. (b) Intensity in heatmap, with red corresponding to high and blue to low expression, with common event that occur in PCa metastasis. (c) Number of metastatic events separated by high, intermediate, and low miR-152 expression. (d) Low miR-152 expression correlated with decrease in probability of biochemical recurrence free survival p=0.0004 (log-rank test).

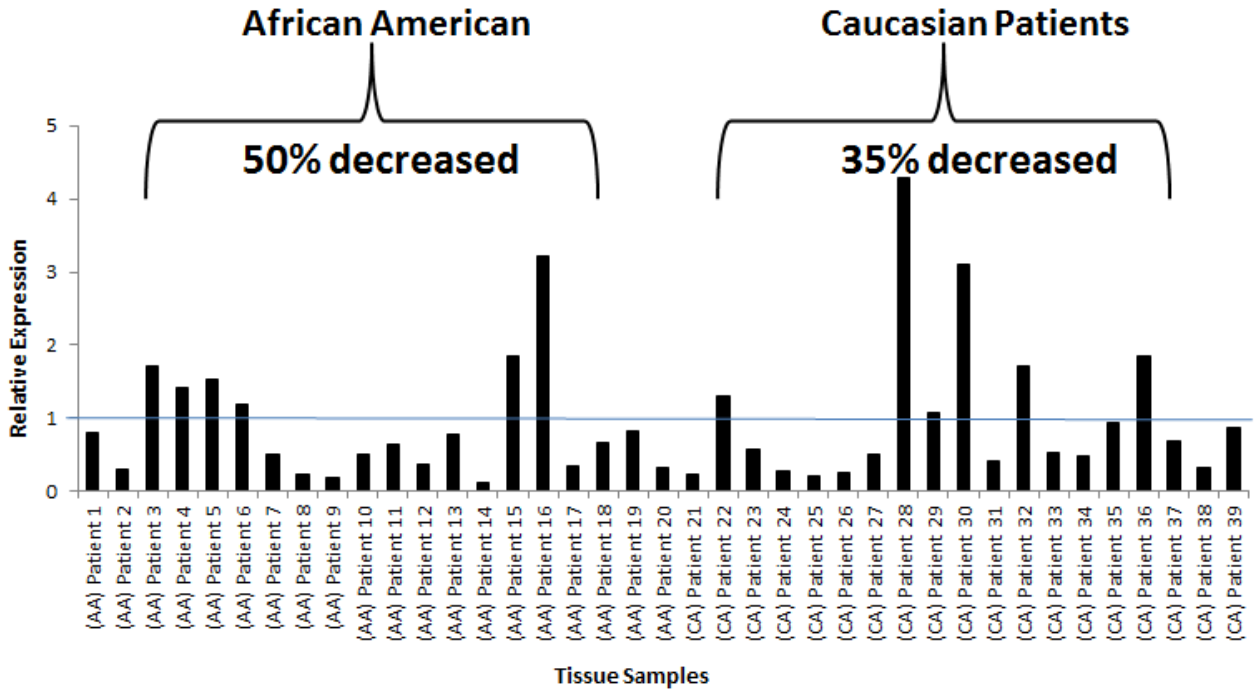

Fig 5: miR-152 expression in AA and CA matched normal tumor cohort. (a) qRT-PCR of miR-152 expression in normal-tumor paired prostate tissue samples. All samples were normalized to the adjacent normal samples. All values under value one represent down-regulation of miR-152. (b) Plot demonstrating the individual miR-152 expression values in AA and CA patients: Note: 50 % of the individual AA patients had significant lower miR-152 expression compared to only 35 % of CA patients. p-values (Benjamini-Hochberg corrected for multiple tests) .

type 3′- UTR) or mutating these sites (DNMT1 Mu 3′-UTR) that contain the putative miR-152 binding sites. All miR-152 transfected cells showed decreased DNMT1 wild-type 3′-UTR luciferase activity, whereas DNMT1 Mu 3′-UTR luciferase activity was not affected (Figure 7c). Since we demonstrated that loss of miR-152 occurs

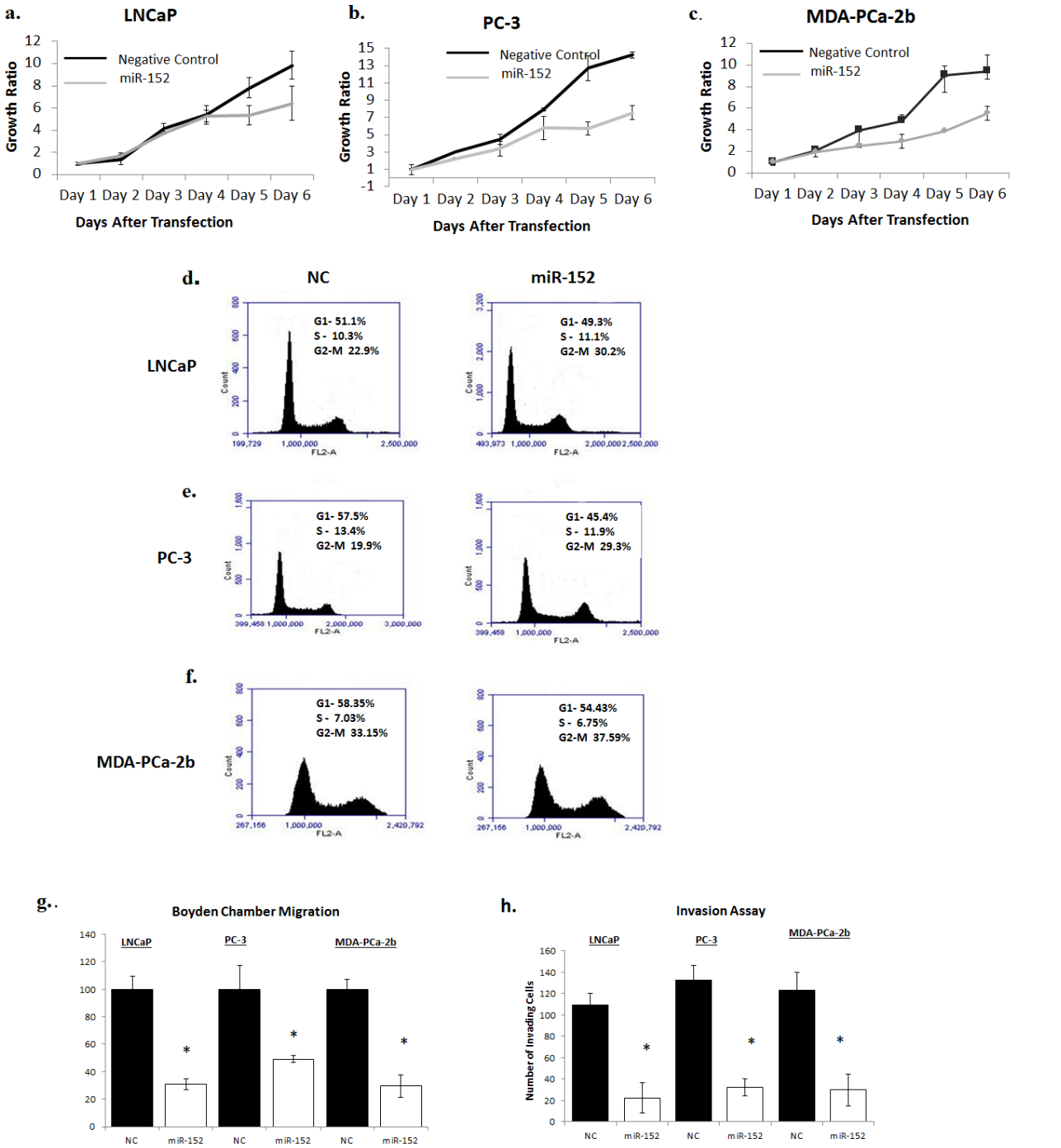

Fig 6: Restoring miR-152 expression decreases cell proliferation, migration, and invasion. (a) Proliferation of LNCaP, (b) PC-3, (c) and MDA-PCa2b cells that were transfected with either 30 nM of miR-152 mimic or miR-NC (negative control) was measured by MTT for 6 days. Results shown are representative of three independent experiments averaged and normalized to Day 1 ± s.e. *p<0.05. (d) LNCaP, (e) PC-3, (f) and MDA-PCa-2b cells were analyzed by flow cytometry after 3 days of miR-152 mimic transfection (30 nM). miR-152 caused G2-M arrest in cell cycle progression in PCa cell lines. Results shown are representative of three independent experiments. (g) Relative cell migration of LNCaP PC-3, and MDA-PCa-2b cells was measured utilizing Boyden migration chambers. Results shown are representative of two individual experiments performed in triplicate. (h) LNCaP, PC-3, and MDA-PCa-2b cells transfected with miR-152 mimic showed a decrease in the number of cells invading through a layer of Matrigel relative to cells treated with miR-NC (negative control). All data presented are the means of three independent experiments ± s.e. *P<0.05.

through promoter methylation, we asked if there was a reciprocal relationship between miR-152 and DNMT1. Treatment of LNCaP, PC-3, and MDA-PCa-2b cells with DNMT1 siRNA caused statistically significant increases in miR-152 expression (Figure 7d).

To examine the possible broader influence that loss of miR-152 has in PCas, we queried the TargetScan *in silico* database to determine additional gene targets that could be regulated by miR-152. Of the top genes, Rictor, TGF-β, SOS1, ABCD3, SMAD4, SOX2, E2F1, and Dicer were predicted. To determine their influence, a custom gene array of these genes was designed (Supplemental Table 5), and expression levels in LNCaP, PC-3, and MDA-PCa-2b cells that were transfected with miR-152 were assayed. Although, the effect of ectopic miR-152 on gene expression varied among the cell lines, we observed consistent decrease expression in Rictor, TGF-β, and SOS1. Interestingly, in the African American derived MDA-PCa-2b, we observed significant decreases in ABCD3 and SOS1, which have been previously reported to be associated with African American prostate tumors [4, 5]. Together, these results indicate that miR-152 regulates epigenetic events that promote tumorigenesis.

DISCUSSION

Numerous studies have now reported gene differences AA and CA prostate tumors [4, 6, 7, 25, 26]. As the field of health disparities is in its infancy, these reports provide the first evidence of population-based genetic contributions to aggressive disease. However, the regulation of these genes is still elusive. To address this question, without influence of non-epithelial stromal cells typically present in tissues, we utilized

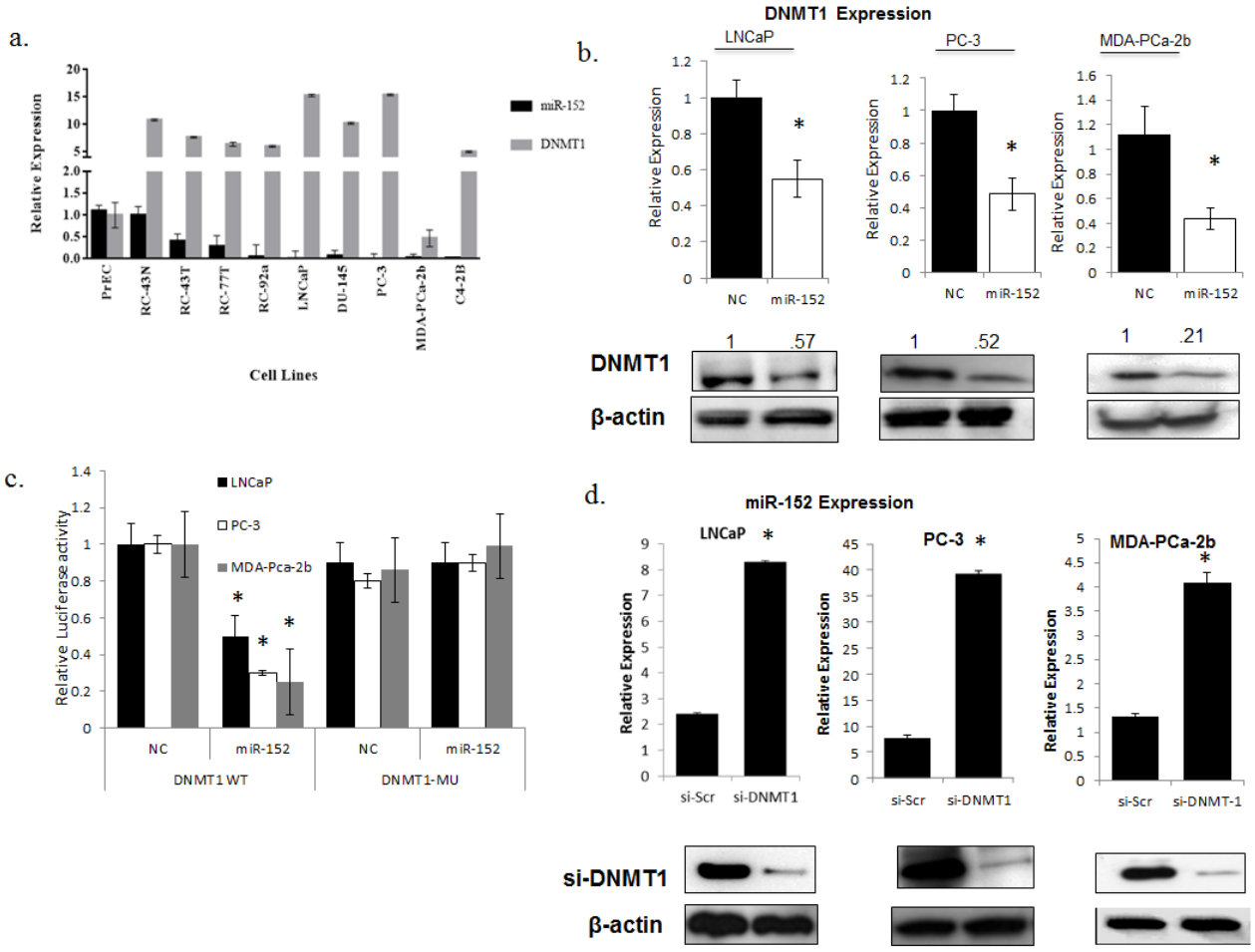

Fig. 7: Comparison of miR-152 and DNMT-1 relationship in PCa cell lines (a) Relative miRNA and mRNA expressions of miR-152 and DNMT1 were determined by qRT-PCR in a panel of prostate cell lines with increasing aggressiveness. (b) miR-152 or scrambled oligonucleotides as NC (negative control) treatment of LNCaP, PC-3, MDA-PCa-2b cells resulted in decreases of DNMT1 at both RNA and protein levels. (c) Dual-luciferase assays were performed for LNCaP, PC-3, and MDA-PCa-2b cells co-transfected with the firefly luciferase constructs containing the DNMT1 wild-type or Mu 3′-UTR and miR-152 mimics or (NC) negative control. (d) siRNA-DNMT1 treatment resulted in increases in miR-152 expression in LNCaP, PC-3, and MDA-PCa-2b cells, as determined by qRT-PCR. DNMT1 expression was analyzed by immunoblots utilizing anti-DNMT1 antibody for both LNCaP, PC-3, a nd MDA-PCa-2b cells after siR-DNMT1 treatment. For all qRT-PCR experiments, expression was normalized to RNU48 (miRNA) and GAPDH (mRNA) controls. All data presented are the means of three independent experiments ± s.e. *P<0.05.

AA- and CA-derived cell lines derived from benign and primary tumors, along with well-established cell lines derived from metastatic PCas. Our findings derived by miRNA microarray analysis revealed a distinct miRNA expression pattern in AA-derived cell lines. qRT-PCR validation of these miRNAs showed that the five most significant miRNAs were decreased in metastatic cell lines, suggesting a role for these molecules in tumorigenesis. Since previous reports have demonstrated inheritable epigenetic changes in AA patients, we sought to determine if decreased expression was the result of DNA methylation. *In silico* analysis revealed that these miRNAs have dense CG regions in the promoter. Further evidence that methylation of CpG islands causes silencing is that each of the miRNAs, albeit to varying degrees, is re-expressed after treatment with 5-aza-2'd or TSA. To our knowledge, this is the first report that demonstrates a methylated miRNA profile that can be associated with the progression of AA prostate tumors.

Of the miRNAs influenced by 5-aza-2'd, several have been found in other tumor types, including PCa. For example, miR-132, which targets both heparin-binding epidermal growth factor and TALIN2, is silenced by hypermethylation [15]. Of the miRNAs we assayed, miR-152 demonstrated the most significant reversal of expression, an effect consistent for both LNCaP and PC-3 cell lines. Previous reports regarding endometrial cancer [23], gastrointestinal cancer [27], and ovarian cancer [28, 29], and a report relating to PCa [30], published during the preparation of this manuscript, show that miR-152 levels are decreased in more advanced tumors. Analysis of patient data from the Taylor et al. study, deposited in the NIH-sponsored Geo database, confirms that miR-152 expression is low in the more advanced primary tumors, with the lowest expression in metastatic samples. However our analysis provides evidence that low miR-152 levels decreases probability of biochemical recurrence free survival in patients. qRT-PCR to measure normal-tumor expression ratios confirmed these findings, with 67% of patients displaying lower miR-152 expression. However, the most relevant observation is that AA patients display decreased expression of miR-152 in both uninvolved and paired tumors compared to CA patients of similar age, stage, and Gleason grade. To determine the mechanism for decreased miR-152, sodium bisulfite modification and sequencing of miR-152 promoter in aggressive PCa cell lines were performed. Both LNCaP and PC-3 cells showed 100% methylation status, highlighting that, in aggressive tumors, hypermethylation of the miR-152 promoter is a mode of silencing miR-152.

miR-152 directly targets the 3′ UTR of DNMT1 [23]. Across our cell line panel, DNMT1 and miR-152 showed an inverse relationship in expression. Although the miR-152/DNMT1 inverse expression relationship was significant in MDA-PCa-2b cells, both the LNCaP and PC-3 cells showed much greater miR-152/DNMT1 expression differences. However in all three cell lines, we confirmed that forced expression of miR-152 results in decreased expression of DNMT1 at both the RNA and protein levels. We also confirmed in LNCaP, PC-3, and MDA-PCa-2b cells decreased expression of several candidate targets that have been implicated in AA prostate tumors. SOS-1, which is a regulator of EGFR expression and downstream signaling, is increased in AA PCas, and most significantly decreased in the AA derived MDA-PCa-2b cells [5]. Although Rictor, a subunit of the mTORC2 complex, has not been directly implicated in AA PCas, the phosphatidylinositol-3-kinase/AKT (PI3K/AKT) pathway, which is a regulator of the mTORC2 complex, has been associated with AA PCas [25]. Whereas TGF-α is a direct target of miR-152 in PCa cell lines [30], we observed decreased TGF-β mRNA expression after forced miR-152 expression in all three cell lines, which further suggests that loss of miR-152 promotes increased aggressiveness through multiple signaling pathways. Previously, we have demonstrated that ABCD3 expression is associated with African American Prostate tumors [4.] Interestingly, we observed decreased ABCD3 expression in the MDA-PCa-2b cells after miR-152 ectopic expression, that was not observed in LNCaP or PC-3 cells. Because DNMT1 has been characterized as one of the main enzymes responsible for maintenance of global methylation patterns in tumor-related genes [31, 32], we investigated the role of DNMT1 on miR-152. We found that depletion of DNMT1 through siRNA resulted in increased miR-152 in both LNCaP, PC-3, and MDA-PCa-2b cell lines, highlighting that the effect is independent of androgen sensitivity. However, there appears to be a feed-forward loop where either loss of miR-152 and/or increased DNMT1 maintains methylation patterns, and hence miR-152 expression. miR-152 is gaining interest as a factor in various tumor types; a recent report concerning nickel sulfide-transformed human bronchial epithelial (16HBE) cells demonstrated that the miRNA-152/DNMT1 relationship develops early in transformed cells [24]. Treatment of cells with 5-aza-2'-d or depletion of DNMT1 led to increased miR-152 expression by reversal of promoter hypermethylation. These findings are similar to those presented here, however the available data relating to PCas suggest that the relationship between loss of miR-152 and increased DNMT1 occurs during the progression to advanced tumor status.

Our finding of a regulatory mechanism that maintains methylation patterns has implications for AA PCa patients. The fact that miR-152 expression is lower in non-malignant tissues from AA patients compared to CA non-malignant tissues suggests that miR-152 expression is regulated by inheritable differences. Although the cause of this decreased expression is still speculative, using NCBI Genome and dpSNP Database (http://www.ncbi.nlm.nih.gov/projects/SNP/snp_ref.cgi?rs=12940701), we did identify 38 single-nucleotide polymorphisms

(SNPs) on chromosome 17q21 (46114527…..46114613, complement1) region where miR-152 is located. Of these, rs200114569, which is associated with a C to G nucleotide change, and rs12940701, which is associated with a C to T change, were of interest because they may affect the methylation status of the miR-152 gene. The rs12940701 SNP has a relatively high frequency (15%) of the minor T allele in the European American population (n=120) relative to the Yoruba (Nigerian) population (n=118). Thus, the European American population could have lower methylation rates since the C nucleotide is changed to the T nucleotide, whereas, in the Yoruba population, this shift is less frequent, allowing for more C nucleotides, thus possibly increasing the rate of methylation. Further analysis should focus on the methylation frequency of miR-152 and on genotyping SNPs that compromise miR-152 expression in AAs and CAs.

In summary, the present work highlights miR-152 as a tumor suppressor that is inactivated by methylation. Because a large number of tumor/metastasis suppressor genes are silenced as a result of methylation, miR-152 could be a central regulator of key events that contribute to tumorigenesis and aggressiveness and thus has the potential to be a therapeutic agent for PCa treatment. These results begin to unravel the molecular mechanism associated with the aggressive tumors of AA patients.

MATERIALS AND METHODS

PCa cell lines and primary tissue samples

Immortalized PCa cell lines RC-77T/E (T3c poorly differentiated primary tumor), RC-77N/E (non-malignant) were derived from AA patient as previously described [21]. RC-43T/E (T4 poorly differentiated primary tumor) and RC-43N/E (non-malignant) were also obtained from an AA patient (characterization unpublished). Benign cell lines derived RC-165N/hTERT (derived from AA patient) [33] and RC-170N/hTERT (derived from CA patient) [34], and primary tumor cell line RC-92a/hTERT (derived from CA patient) cells [35]. All cell lines were cultured in keratinocyte serum-free medium (KGM, LifeTechnologies, Carlsbad, CA) supplemented with bovine pituitary extract, recombinant epidermal growth factor, and 1% penicillin-streptomycin-neomycin were maintained in KGM medium as previously described [36]. Non-malignant CA prostate epithelial cells (PrEC) were obtained from Clonetics Lonza (Switzerland) and maintained in Prostate Epithelial Cell Growth Medium (Clonetics). The CA androgen-independent and metastatic PC-3 and DU-145 PCa cell lines were maintained in Dulbecco's Modified Eagle medium (DMEM) supplemented with 10% fetal bovine serum and 1% penicillin-streptomycin-neomycin. The CA LNCaP and C4-2b androgen-dependent and -independent, respectively, prostate cells were maintained in T-medium. RWPE-1 normal prostate cells were maintained in KGM as previously described [37]. The malignant, androgen-receptor positive AA MDA-PCa-2b cells were purchased from ATCC (Manassas, VA). These cells were maintained in F-12K medium supplemented with 20% fetal bovine serum, 25 ng/ml cholera toxin, 10 ng/ml mouse epidermal growth factor, 5 μM phosphoethanolamine, 100 pg/ml hydrocortisone, 45 nM selenious acid, and 5 μg/ml bovine insulin.

Patient Samples

Patient samples were obtained from the Cooperative Human Tissue Network at the University of Alabama at Birmingham (UAB) under Institutional Review Board-approved protocols. Additionally, the Institutional Review Boards of Tuskegee University and UAB approved the use of tissues for this study. Tumor sections were macro dissected. There was no significant difference between the two groups with respect to tumor content. (Average percentages of tumor for AA and CA biopsies were both 54%.) Paired normal tissues were also collected from the same patients. Altogether, samples from each of the 20 AA and 19 CA patients, along with patient-matched normal adjacent tissues, were used for qRT-PCR validation. p-values were generated using graph pad software. T-tests (the Benjamini-Hochberg corrected for multiple tests that reflects the individual patients with significant difference in mir152 expression relative to global mean of u48 for Ct values and global mean for delta Ct values) were performed to test for significant differences between the means, and F-tests were used to assess differences in variance between experimental groups.

Quantitative Real-time PCR (qRT-PCR)

Total RNA extraction was performed using the Ambion recover all nucleic acid isolation kit (AM 1975) modified by replacing filters with (AM10066G). RNA (10 ng) was reverse transcribed using TaqMan miRNA reverse transcription kits (Life Technologies). For mRNA expression, 1 μg of total RNA was reverse transcribed using High Capacity cDNA kits (Invitrogen). Relative expression of miRNAs and mRNA was quantified with the TaqMan Universal PCR Master Mix, No AmpErase UNG, with the 7500 Fast Real-Time PCR system (Life Technologies). Thermal cycling conditions included enzyme activation for 10 min at 95°C, 40 cycles of 95°C for 15 s, and 60°C for 60 s, according to provider's protocol. Reverse transcription for mRNA was accomplished as previously described [22, 38]. SYBR Green reagents (Invitrogen) were used for quantitative real-time PCR. Thermal cycling conditions for primer sequences used for mRNA detection are included in

the table below . Analyses for miRNA and mRNA were performed in triplicate. RNU48 miRNA, GAPDH, and 18S ribosomal RNA were used as endogenous controls.

Transfection of miRNA Precursor

LNCaP, PC-3, and MDA-PCa-2b PCa cell lines were seeded at 2 x 10^5 cells in six-well plates on the day before transfection. Lipofectamine 2000 reagent (Life Technologies) was used to transfect 5-15 nmol of miR-152 or 5-15 nmol of miR-Negative Control #1 in Opti-MEM (Life Technologies). Cells were harvested for assays three days after recovery in fully supplemented media, as described previously [38].

Cell Proliferation Assays

LNCaP, PC-3, and MDA-PCa-2b cells (2.5 x 102) were plated in 96-well plates in DMEM. After being cultured for 24 hr, cells were transfected with miR-152 or Negative Control #1 (Life Technologies) at a concentration of 30 nM. Cell viability was determined at 24, 48, 72, 96, and 120 days after transfection. All cells were incubated with 10 µl of 3-(4,5-dimethylthiazol-2-yl)-2,5-diphenyltetrazolium bromide (MTT, Sigma-Aldrich, St. Louis, MO) solution (5 mg/ml) in PBS for 4 hr. Dimethylsulfoxide (50 µl) was added for 10 min after aspiration of the MTT solution. Plates were read at 560 nm.

Cell Migration and Invasion assay

Cell migration and invasion was determined using the Boyden chamber assay. Briefly, 20,000 cells were plated in the upper chamber, with or without Matrigel, containing serum-free medium containing 1% bovine serum albumin for 24 hours; this then was replaced with a serum-free medium for an additional 24 hours. The lower chamber contained medium with 10 ng/mL of epidermal growth factor was used as a chemo-attractant. The number of cells that migrated or invaded through the matrix over a 48 hour-period was determined by counting cells that stained with crystal violet on the bottom of the filter. All experiments were performed in triplicate.

Sodium Bisulfite Modification and Methylation Analysis

DNA was extracted with GenElute Mammalian Genomic DNA Miniprep kits (Sigma-Aldrich) following the manufacturer's instructions. Subsequently, bisulfite conversion of DNA (2 µg) was performed with EpiTect Bisulfite kits (Qiagen, Valencia, CA). The miR-152 sequence was determined by using the UCSC Genome Browser [39]. Methylation PCR amplification primers for sequencing were designed using MethPrimer [40]. Sequence from 5' to 3' - Primer 1: GGGTTAGGGGGAGTAGTTAATTTAG and Primer 2: ATAAACTCCAAAAACATACCCATCA. qRT-PCR was performed on bisulfite-converted DNA (1 µl), using the primers described above covering two CpG regions upstream from the miR-152 promoter DNA sequence. A second round of amplification was performed on the first PCR amplicons and subsequently characterized by electrophoresis on 1.2% agarose gels. Sequencing of amplicons was performed at the UAB Heflin Center, Birmingham, AL. Bisulfite sequencing was analyzed by an online DNA methylation platform, Bisulfite Sequencing Data and Presentation Compilation (http://biochem.jacobs-university.de/BDPC/).

Immunoblots

Cells were harvested 3 days after miR-152 transfection, washed with PBS, and lysed in NP-40 lysis buffer [10 mM Tris-Cl (pH 7.4), 10 mM NaCl, 3 mM $MgCl_2$ 0.5% NP-40 (Nonidet P-40), 0.15 mM spermine, 0.5 mM spermidine, and protease inhibitor solution] and centrifuged at 12,000 g for 10 min at 4°C. Protein concentrations were determined with the BCA Protein Assay kit (Thermo Scientific, Rockford, IL) according to manufacturer's instructions. Protein samples were separated on 7.5% SDS-PAGE pre-cast gels (Thermo Scientific). Protein levels were detected by anti-DNMT1, anti-mTOR, and anti-Rictor rabbit polyclonal antibodies (Cell Signaling, Danvers, MA), and analyzed by chemiluminescence.

Treatment with 5-aza-2'-d

Cells (60% confluent) were treated with 5 µM 5-aza-2'd for 5 days, with fresh media supplemented with 5-aza-2'd every day. Trichostatin A (TSA, a histone deacetylase inhibitor) was administered at a concentration of 100 nM on the last day of treatment. Cells were harvested and assayed for miR-152 expression by qRT-PCR as previously described [21, 22].

Flow Cytometry Analysis

Cells were harvested 3 days after miR-152 transfection, washed with cold PBS, fixed, and permeabilized with 70% cold ethanol for propidium iodide staining. Cell cycle analysis was performed with a flow cytometer (Accuri, Ann Arbor, MI).

miRNA microarray samples

For miRNA expression profiling, 11 unique cell lines were utilized; specifically, PrEC, RC-77N/E, RC-77T/E, RC-43T/E, RC-43N/E, RC-165N/hTERT, RC-92a/hTERT, RC-170N/hTERT, PC-3, MDA-PCa-2b, and C42B. Microarray hybridizations were performed in triplicate for each line by Ausurgen, Austin TX). In addition, primary tumor samples (n=9) were also processed for microarray hybridization (RC-30T, RC-33T, RC-136T, RC-139T, RC-28T, RC-78T, RC-143T, RC-145T and RC-25T). Clinical characteristics are listed in (supplemental table 4). The protocols for RNA extraction and miRNA microarray hybridizations were performed by an outside vendor (Asuragen, Austin, TX).

Raw data processing from microarrays

For data processing, the bioconductor packages pipelined through R interfaces DaNTE [41] and CARMA [42] were used. Pre-processing and normalization was completed with the Affy package. Two distinct array platforms were used during the course of this project; cell lines were hybridized to one platform and primary samples were hybridized to another. The platforms differ in probe content and replication. Arrays of identical platforms were quantile normalized to minimize inter-array noise [43], using the gcRMA method [44]. Subsequently, replicates were merged into median values for statistical association analyses.

Statistical analysis of normalized data

For all analyses, p-values <0.05 were considered as significant. Initial differential expression was detected using an ANOVA linear model. Of the miRNA genes that showed significant variance, we measured the specific differential expression among categorical groupings; diagnosis, pathological stage, and race. Differential expression associated with categories was measured using a moderated T-test in the limma package of R. Cells lines representing tumor and uninvolved from the same individuals were grouped into two categories; Malignant or Non-malignant. This grouping also included established laboratory cell lines (PREC, PC3 and C42b). We incorporated multiple hypothesis testing to correct for false positive (type 1 errors) and false negative (type 2 errors). Specifically, we implemented adjusted p-values (Bonferroni) and false discovery rates (FDR) using the Benjamini and Hochberg method [45]. A moderate 10% FDR cutoff was used when applicable. We also used hierarchical clustering analyses to determine groups of differentially expressed miRNAs between specific variables and to isolate specific nodes of probes that shared similar expression trends.

We used non-parametric tests when comparing across array platforms to validate the significance of specific factors in a given variable category. Specifically, a Kruskal-Walis test was used for all variables. In addition, for variables with only 2 levels, a Wilcoxon Rank Sum test was utilized for secondary validation. In cases where strict fold change values were of importance, the fold change between two factor levels was calculated using the ratio of mean expression between the variables over differences in expression between the variables. [log(x/y) = log(x) - log(y)].

To determine the ability of significant probe profiles to differentiate samples into relevant categories, we used a partial least squares (PLS) principle component test. Specifically, once probes were found to be significantly differentially expressed, following hierarchical clustering, we identified suitable nodes or combination of probes, for each category. We determined differentially expressed probes based on diagnosis, stage and as the predictors and miRNA expression values as the response. These tests both determined whether the probes statistically associated with a specific variable or had predictive value across independent primary samples not utilized in the initial discovery ANOVA and non-parametric tests. If the largest percent variation could be explained by the variable extracted/tested, and the samples segregated according to proper category variable annotation, the probe set was considered to have significant predictive value for the specified categories. For these analyses, the DAnTE 1.2 program was utilized.

Competing interests

The authors have no conflicting financial interests.

Authors' contributions

ST and CY conceived, designed, performed the experiments, and analyzed the data. MD performed statistical analysis on microarrays and patient samples. HW, TT, and FZ performed experiments. WJ, GZ generated miRNA-mRNA binding constructs. ST, WG and CY wrote the manuscript. All authors have read and approve the manuscript in its final form.

ACKNOWLEDGMENTS

This work was supported by grants G12 RR03059-21A1 (NIH/RCMI) [CY], U54 CA118623 (NIH/NCI) [CY]; and a Department of Defense Grants, PC120913, W81XWH-10-1-0543. Statistical analysis from the Geo website was performed by both the University Alabama at Birmingham and Tuskegee University Statistical Cores. We would also like to thank members of the Yates

laboratory for their comments and discussions.

REFERENCES

1. Kheirandish P and Chinegwundoh F. Ethnic differences in prostate cancer. British journal of cancer. 105(4):481-485.
2. Caso JR, Tsivian M, Mouraviev V, Polascik TJ and Moul JW. Pathological T2 sub-divisions as a prognostic factor in the biochemical recurrence of prostate cancer. BJU international. 106(11):1623-1627.
3. Powell IJ, Dyson G, Land S, Ruterbusch J, Bock CH, Lenk S, Herawi M, Everson RB, Giroux CN, Schwartz AG and Bollig-Fischer A. Genes associated with prostate cancer are differentially expressed in African American and European American men. Cancer Epidemiol Biomarkers Prev.
4. Reams RR, Kalari KR, Wang H, Odedina FT, Soliman KF and Yates C. Detecting gene-gene interactions in prostate disease in African American men. Infectious agents and cancer. 6 Suppl 2:S1.
5. Timofeeva OA, Zhang X, Ressom HW, Varghese RS, Kallakury BV, Wang K, Ji Y, Cheema A, Jung M, Brown ML, Rhim JS and Dritschilo A. Enhanced expression of SOS1 is detected in prostate cancer epithelial cells from African-American men. Int J Oncol. 2009; 35(4):751-760.
6. Reams RR, Agrawal D, Davis MB, Yoder S, Odedina FT, Kumar N, Higginbotham JM, Akinremi T, Suther S and Soliman KF. Microarray comparison of prostate tumor gene expression in African-American and Caucasian American males: a pilot project study. Infectious agents and cancer. 2009; 4 Suppl 1:S3.
7. Wallace TA, Prueitt RL, Yi M, Howe TM, Gillespie JW, Yfantis HG, Stephens RM, Caporaso NE, Loffredo CA and Ambs S. Tumor immunobiological differences in prostate cancer between African-American and European-American men. Cancer research. 2008; 68(3):927-936.
8. Kim JH, Dhanasekaran SM, Prensner JR, Cao X, Robinson D, Kalyana-Sundaram S, Huang C, Shankar S, Jing X, Iyer M, Hu M, Sam L, Grasso C, Maher CA, Palanisamy N, Mehra R, et al. Deep sequencing reveals distinct patterns of DNA methylation in prostate cancer. Genome research. 21(7):1028-1041.
9. Kobayashi Y, Absher DM, Gulzar ZG, Young SR, McKenney JK, Peehl DM, Brooks JD, Myers RM and Sherlock G. DNA methylation profiling reveals novel biomarkers and important roles for DNA methyltransferases in prostate cancer. Genome research. 21(7):1017-1027.
10. Enokida H, Shiina H, Urakami S, Igawa M, Ogishima T, Pookot D, Li LC, Tabatabai ZL, Kawahara M, Nakagawa M, Kane CJ, Carroll PR and Dahiya R. Ethnic group-related differences in CpG hypermethylation of the GSTP1 gene promoter among African-American, Caucasian and Asian patients with prostate cancer. Int J Cancer. 2005; 116(2):174-181.
11. Kwabi-Addo B, Wang S, Chung W, Jelinek J, Patierno SR, Wang BD, Andrawis R, Lee NH, Apprey V, Issa JP and Ittmann M. Identification of differentially methylated genes in normal prostate tissues from African American and Caucasian men. Clin Cancer Res. 16(14):3539-3547.
12. Friedman RC, Farh KK, Burge CB and Bartel DP. Most mammalian mRNAs are conserved targets of microRNAs. Genome research. 2009; 19(1):92-105.
13. Lopez-Serra P and Esteller M. DNA methylation-associated silencing of tumor-suppressor microRNAs in cancer. Oncogene. 31(13):1609-1622.
14. Negrini M, Nicoloso MS and Calin GA. MicroRNAs and cancer--new paradigms in molecular oncology. Current opinion in cell biology. 2009; 21(3):470-479.
15. Formosa A, Lena AM, Markert EK, Cortelli S, Miano R, Mauriello A, Croce N, Vandesompele J, Mestdagh P, Finazzi-Agro E, Levine AJ, Melino G, Bernardini S and Candi E. DNA methylation silences miR-132 in prostate cancer. Oncogene. 32(1):127-134.
16. Suh SO, Chen Y, Zaman MS, Hirata H, Yamamura S, Shahryari V, Liu J, Tabatabai ZL, Kakar S, Deng G, Tanaka Y and Dahiya R. MicroRNA-145 is regulated by DNA methylation and p53 gene mutation in prostate cancer. Carcinogenesis. 32(5):772-778.
17. Lodygin D, Tarasov V, Epanchintsev A, Berking C, Knyazeva T, Korner H, Knyazev P, Diebold J and Hermeking H. Inactivation of miR-34a by aberrant CpG methylation in multiple types of cancer. Cell cycle (Georgetown, Tex. 2008; 7(16):2591-2600.
18. Jones J, Grizzle W, Wang H and Yates C. MicroRNAs that affect prostate cancer: emphasis on prostate cancer in African Americans. Biotech Histochem.
19. White NM, Youssef YM, Fendler A, Stephan C, Jung K and Yousef GM. The miRNA-kallikrein axis of interaction: a new dimension in the pathogenesis of prostate cancer. Biological chemistry. 393(5):379-389.
20. Brase JC, Johannes M, Schlomm T, Falth M, Haese A, Steuber T, Beissbarth T, Kuner R and Sultmann H. Circulating miRNAs are correlated with tumor progression in prostate cancer. International journal of cancer. 128(3):608-616.
21. Theodore S, Sharp S, Zhou J, Turner T, Li H, Miki J, Ji Y, Patel V, Yates C and Rhim JS. Establishment and characterization of a pair of non-malignant and malignant tumor derived cell lines from an African American prostate cancer patient. Int J Oncol. 37(6):1477-1482.
22. Theodore SC, Rhim JS, Turner T and Yates C. MiRNA 26a expression in a novel panel of African American prostate cancer cell lines. Ethn Dis. 20(1 Suppl 1):S1-96-100.
23. Tsuruta T, Kozaki K, Uesugi A, Furuta M, Hirasawa A, Imoto I, Susumu N, Aoki D and Inazawa J. miR-152 is a tumor suppressor microRNA that is silenced by DNA hypermethylation in endometrial cancer. Cancer research. 71(20):6450-6462.
24. Ji W, Yang L, Yuan J, Yang L, Zhang M, Qi D, Duan

X, Xuan A, Zhang W, Lu J, Zhuang Z and Zeng G. MicroRNA-152 targets DNA methyltransferase 1 in NiS-transformed cells via a feedback mechanism. Carcinogenesis. 34(2):446-453.

25. Wang BD, Yang Q, Ceniccola K, Bianco F, Andrawis R, Jarrett T, Frazier H, Patierno SR and Lee NH. Androgen receptor-target genes in african american prostate cancer disparities. Prostate cancer. 2013:763569.
26. Jones J, Grizzle W, Wang H and Yates C. MicroRNAs that affect prostate cancer: emphasis on prostate cancer in African Americans. Biotech Histochem. 2013; (2013 The Biological Stain Commission):1-15.
27. Chen Y, Song Y, Wang Z, Yue Z, Xu H, Xing C and Liu Z. Altered expression of MiR-148a and MiR-152 in gastrointestinal cancers and its clinical significance. J Gastrointest Surg. 14(7):1170-1179.
28. Xiang Y, Ma N, Wang D, Zhang Y, Zhou J, Wu G, Zhao R, Huang H, Wang X, Qiao Y, Li F, Han D, Wang L, Zhang G and Gao X. MiR-152 and miR-185 co-contribute to ovarian cancer cells cisplatin sensitivity by targeting DNMT1 directly: a novel epigenetic therapy independent of decitabine. Oncogene.
29. Zhou X, Zhao F, Wang ZN, Song YX, Chang H, Chiang Y and Xu HM. Altered expression of miR-152 and miR-148a in ovarian cancer is related to cell proliferation. Oncology reports. 27(2):447-454.
30. Zhu C, Li J, Ding Q, Cheng G, Zhou H, Tao L, Cai H, Li P, Cao Q, Ju X, Meng X, Qin C, Hua L, Shao P and Yin C. miR-152 controls migration and invasive potential by targeting TGFalpha in prostate cancer cell lines. The Prostate.
31. Gravina GL, Ranieri G, Muzi P, Marampon F, Mancini A, Di Pasquale B, Di Clemente L, Dolo V, D'Alessandro AM and Festuccia C. Increased levels of DNA methyltransferases are associated with the tumorigenic capacity of prostate cancer cells. Oncology reports. 29(3):1189-1195.
32. Yaqinuddin A, Qureshi SA, Qazi R, Farooq S and Abbas F. DNMT1 silencing affects locus specific DNA methylation and increases prostate cancer derived PC3 cell invasiveness. The Journal of urology. 2009; 182(2):756-761.
33. Gu Y, Kim KH, Ko D, Srivastava S, Moul JW, McLeod DG and Rhim JS. Androgen and androgen receptor antagonist responsive primary African-American benign prostate epithelial cell line. Anticancer research. 2005; 25(1A):1-8.
34. Li H, Zhou J, Miki J, Furusato B, Gu Y, Srivastava S, McLeod DG, Vogel JC and Rhim JS. Telomerase-immortalized non-malignant human prostate epithelial cells retain the properties of multipotent stem cells. Experimental cell research. 2008; 314(1):92-102.
35. Miki J, Furusato B, Li H, Gu Y, Takahashi H, Egawa S, Sesterhenn IA, McLeod DG, Srivastava S and Rhim JS. Identification of putative stem cell markers, CD133 and CXCR4, in hTERT-immortalized primary nonmalignant and malignant tumor-derived human prostate epithelial cell lines and in prostate cancer specimens. Cancer research. 2007; 67(7):3153-3161.
36. Gu Y, Kim KH, Ko D, Nakamura K, Yasunaga Y, Moul JW, Srivastava S, Arnstein P and Rhim JS. A telomerase-immortalized primary human prostate cancer clonal cell line with neoplastic phenotypes. International journal of oncology. 2004; 25(4):1057-1064.
37. Bello D, Webber MM, Kleinman HK, Wartinger DD and Rhim JS. Androgen responsive adult human prostatic epithelial cell lines immortalized by human papillomavirus 18. Carcinogenesis. 1997; 18(6):1215-1223.
38. Jones J, Wang H, Zhou J, Hardy S, Turner T, Austin D, He Q, Wells A, Grizzle WE and Yates C. Nuclear Kaiso indicates aggressive prostate cancers and promotes migration and invasiveness of prostate cancer cells. The American journal of pathology. 181(5):1836-1846.
39. Kent WJ, Sugnet CW, Furey TS, Roskin KM, Pringle TH, Zahler AM and Haussler D. The human genome browser at UCSC. Genome research. 2002; 12(6):996-1006.
40. Li LC and Dahiya R. MethPrimer: designing primers for methylation PCRs. Bioinformatics (Oxford, England). 2002; 18(11):1427-1431.
41. Polpitiya AD, Qian WJ, Jaitly N, Petyuk VA, Adkins JN, Camp DG, 2nd, Anderson GA and Smith RD. DAnTE: a statistical tool for quantitative analysis of -omics data. Bioinformatics (Oxford, England). 2008; 24(13):1556-1558.
42. Greer KA, McReynolds MR, Brooks HL and Hoying JB. CARMA: A platform for analyzing microarray datasets that incorporate replicate measures. BMC bioinformatics. 2006; 7:149.
43. Smyth GK and Speed T. Normalization of cDNA microarray data. Methods (San Diego, Calif. 2003; 31(4):265-273.
44. Hsieh WP, Chu TM, Lin YM and Wolfinger RD. Kernel density weighted loess normalization improves the performance of detection within asymmetrical data. BMC bioinformatics. 12:222.
45. Benjamini Y, Drai D, Elmer G, Kafkafi N and Golani I. Controlling the false discovery rate in behavior genetics research. Behavioural brain research. 2001; 125(1-2):279-284.

informa
healthcare

The effects of frozen tissue storage conditions on the integrity of RNA and protein

H Auer[1], JA Mobley[2], LW Ayers[3], J Bowen[4], RF Chuaqui[5], LA Johnson[3], VA Livolsi[6], IA Lubensky[5], D McGarvey[6], LC Monovich[4], CA Moskaluk[7], CA Rumpel[7], KC Sexton[8], MK Washington[9], KR Wiles[9], WE Grizzle[8], NC Ramirez[4]

[1]*Functional Genomics Core, Institute for Research in Biomedicine, Barcelona, Spain,* [2]*Department of Surgery, University of Alabama at Birmingham, Birmingham, Alabama,* [3]*Department of Pathology, The Ohio State University, Columbus, Ohio,* [4]*Department of Pathology and Laboratory Medicine, Nationwide Children's Hospital, Columbus, Ohio,* [5]*National Cancer Institute, Cancer Diagnosis Program, Pathology Investigations and Resources Branch (PIRB), Rockville, Maryland,* [6]*Hospital of the University of Pennsylvania, Philadelphia, Pennsylvania,* [7]*Department of Pathology, University of Virginia, Charlottesville, Virginia,* [8]*Department of Pathology, University of Alabama at Birmingham, Birmingham, Alabama, and* [9]*Vanderbilt University Medical Center, Nashville, Tennessee*

Accepted January 15, 2014

Biotech Histochem Downloaded from informahealthcare.com by Dr. G.S. Nettleton on 06/25/14
For personal use only.

Abstract

Unfixed tissue specimens most frequently are stored for long term research uses at either −80° C or in vapor phase liquid nitrogen (VPLN). There is little information concerning the effects such long term storage on tissue RNA or protein available for extraction. Aliquots of 49 specimens were stored for 5–12 years at −80° C or in VPLN. Twelve additional paired specimens were stored for 1 year under identical conditions. RNA was isolated from all tissues and assessed for RNA yield, total RNA integrity and mRNA integrity. Protein stability was analyzed by surface-enhanced or matrix-assisted laser desorption ionization time of flight mass spectrometry (SELDI-TOF-MS, MALDI-TOF-MS) and nano-liquid chromatography electrospray ionization tandem mass spectrometry (nLC-ESI-MS/MS). RNA yield and total RNA integrity showed significantly better results for −80° C storage compared to VPLN storage; the transcripts that were preferentially degraded during VPLN storage were these involved in antigen presentation and processing. No consistent differences were found in the SELDI-TOF-MS, MALDI-TOF-MS or nLC-ESI-MS/MS analyses of specimens stored for more than 8 years at −80° C compared to those stored in VPLN. Long term storage of human research tissues at −80° C provides at least the same quality of RNA and protein as storage in VPLN.

Key words: assays, human tissues, proteomics, RNA, storage, temperatures

The current gold standard for preservation of RNA and protein analytes in tissue specimens is snap-freezing, with subsequent storage in either mechanical freezers at −80° C or in the vapor phase of liquid nitrogen (VPLN). Although RNA and protein can be isolated from tissue specimens processed for routine histologic analysis (formalin fixation and paraffin embedding), the processing can cause alterations in RNA and proteins; however, there is little difference in assay results when mRNA is analyzed by real-time, reverse transcriptase quantitative polymerase chain reaction technology (RT-Q-PCR) (Steg et al. 2006, 2007). Frozen samples of tissues, however, are preferred for some basic and translational studies, especially genome-wide sequencing experiments. Long term storage of samples sometimes is desirable, because the research value of human specimens, especially

Correspondence: William E. Grizzle, M.D., Ph.D., University of Alabama at Birmingham Department of Pathology, Division of Anatomic Pathology, ZRB 408, 1720 Second Avenue South, Birmingham, AL 35294. Phone: (205) 934-4214, Fax: (205) 975-7128, e-mail: wgrizzle@uab.edu
© 2014 The Biological Stain Commission
Biotechnic & Histochemistry 2014, **Early Online: 1–11.**

DOI: 10.3109/10520295.2014.904927

cancer specimens, increases over time if needed for longitudinal clinical and outcome data.

It is considered a theoretical advantage to store tissue below the glass transition phase of pure water, because aqueous based chemical reactions are thought to cease at the glass transition temperature (T_g). Such conditions are achieved in VPLN (−150º C) and by some mechanical freezers. Owing to logistics and expense, however, many investigators and biorepositories store samples in mechanical freezers at temperatures of −70 to −90° C. It is noteworthy that there is controversy about the exact T_g value of pure water; recent studies suggest that this is 165° K or −108° C, although it frequently is reported to be 136° K or −137° C (Giovambattista et al. 2004). Complicating this issue is the fact that cells are not filled with "pure" water, so the practical T_g values for the water in mammalian tissues are unknown. Nevertheless, enzymatic reactions, in general, are thought to continue at −80° C and cells do not remain viable when stored at −80° C.

To compare the relative effects of the two time-honored methods for storing frozen tissue on RNA and protein integrity, we performed a series of analyses to assess the content and quality of the RNA transcripts and proteins/peptides on a cohort of matched human tissue specimens stored for a number of years at both −80° C and in VPLN.

Biotech Histochem Downloaded from informahealthcare.com by Dr. G.S. Nettleton on 06/25/14
For personal use only.

Materials and methods

Patients and specimens

Our study was approved by the Nationwide Children's Hospital Institutional Review Board. The requirement for written informed consent from the participants was waived, because the study used de-identified specimens.

Aliquots of 49 paired human tissue specimens were stored at −80° C in mechanical freezers and matched aliquots were stored in VPLN. An additional 12 paired specimens were obtained from the member institutions of the Cooperative Human Tissue Network (CHTN) and were stored similarly in different types of freezers. The specimens were remnant solid tissues from surgeries that were available after clinical diagnoses had been made. Tumors, normal appearing tissues adjacent to tumors and other non-neoplastic tissue specimens were used (Table 1). The selection of specimens for the first cohort was based on the availability of matched frozen tissue stored in VPLN and at −80° C. The specimens obtained from the CHTN were procured prospectively for this analysis. All tissues were reviewed by pathologists to ensure that the matched specimens from both storage methods were the same histologically (see Specimen Processing section).

The tissue procured from the CHTN were obtained within 2 h of removal from the patient, split into identical aliquots, snap frozen or snap frozen in OCT, then shipped to a central facility on dry ice for storage at either −80° C or in VPLN for 1 year. All freezers used for this study were monitored electronically and manually and no failures in temperature maintenance occurred during the storage of the specimens.

Specimen processing for RNA isolation

Specimens not initially frozen in OCT were embedded by placing the frozen tissue in partially frozen OCT, covering with additional OCT, and freezing at −20° C immediately prior to analysis. All OCT embedded specimens were equilibrated at −20° C, histologic sections were cut using a cryostat, and the sections were stained with hematoxylin and eosin (H & E) for histologic assessment. Ten additional 10 μm frozen sections were obtained and placed on dry ice for isolation of either mRNA or protein.

For RNA isolation, the samples were incubated for 10 min in 1 ml Tri Reagent (Molecular Research Center, Inc., Cincinnati, OH) at 50° C and insoluble material was pelleted by centrifugation for 10 min at 3,000 × g. Nine hundred microliters of supernatant were used for RNA isolation according to the manufacturer's recommendations. Each of the resulting RNA pellets was dissolved in 25 μl RNAse-free water. RNA was quantified using a Nanodrop ND-1000 spectrophotometer (Nanodrop Technologies, Wilmington, DE).

Quantification of total RNA integrity

For microcapillary electrophoresis measurements of total RNA integrity, the Agilent 2100 Bioanalyzer was used in conjunction with the RNA 6000 Nano LabChip kits (Agilent, Waldbronn, Germany) following the manufacturer's recommendations. Bioanalyzer electrophoresis report files were analyzed for RNA integrity number (RIN) and degradation factor as described earlier (Auer et al. 2003). For RIN analysis, 2100 Expert software version B.02.03.SI307 (Agilent) was used. RIN reports total RNA integrity on a scale of 1 to 10, where 1 represents complete degradation and 10 is the highest level of RNA integrity. A value of

Table 1. Tissue types used to assess RNA integrity after long term storage at −80° C and in VPLN

Tissue	Storage period (years)	Tissue	Storage period (years)
thyroid papillary carcinoma	10	choroid plexus carcinoma	8
lymphoma	10	neuroblastoma	8
benign neural tumor	10	colon-non neoplastic	8
dysgerminoma	10	lipoma	8
ganglioglioneuroma	10	hepatoblastoma	8
pilocytic astrocytoma	10	neuroblastoma	8
PNET	10	cellular fibroadenoma breast	8
embryonal rhabdomyosarcoma	10	neuroblastoma	8
ganglioglioneuroma	10	skull mass	8
spleen, normal	10	myxoid neoplasm-malignant	8
endodermal sinus tumor	10	Langerhans histiocytosis	8
pancreatic cystic/solid papillary neoplasm	9	neurofibroma	8
pilocytic astrocytoma	9	neuroblastoma	8
hepatoblastoma	9	paraganglioma	7
ganglioglioneuroma	9	ependymoma	7
neuroblastoma	9	kidney- non neoplastic	7
ganglioneuroma	9	Burkitt's lymphoma	7
lymph node, follicular hyperplasia	9	meningioma	6
spleen, non-neoplastic	9	pilocytic astrocytoma	6
MPNST	9	ependymoma	6
alveolar rhabdomyosarcoma	9	papillary thyroid carcinoma	6
ganglioglioneuroma	9	Burkitt's lymphoma	6
infantile myofibromatosis	9	osteosarcoma	6
neuroblastoma	9	ganglioglioma	5
pilocytic astrocytoma	8		

Biotech Histochem Downloaded from informahealthcare.com by Dr. G.S. Nettleton on 06/25/14
For personal use only.

1 (lowest integrity) was used for samples where no RIN values were available. For degradation factor analysis, results of individual samples were exported from the 2100 Expert software as CSV files and analyzed by Degradometer software version 1.4.2 (Auer et al. 2003). Degradation factor reports total RNA integrity on a scale of 1 to 100, where 1 is the highest level of RNA integrity and 100 is complete degradation. For samples where no degradation factors were available, 100 (lowest integrity) was used for further calculations.

Microarray expression profiling

Samples were used for expression profiling if both of the following criteria were met: 1) at least one of the paired samples showed RIN >1, and 2) at least one of the paired samples showed a degradation factor <100. From 37 paired samples that met these criteria, 25 ng of total RNA per sample were processed using isothermal SPIA Biotin System (NuGEN Technologies, Inc., San Carlos, CA) amplification; 2.2 μg cDNA resulting from the amplification were used for microarray hybridization (Affymetrix Human U133A2.0 GeneChips, Santa Clara, CA).The U133A2.0 microarray contains more than 22,000 probe sets to analyze 18,400 transcripts including 14,500 well-characterized genes. After 16 h hybridization at 45° C, washing and staining of microarrays was performed using a Fluidics Station 450 (Affymetrix); GeneChips were scanned in a GeneChip Scanner 3000 (Affymetrix). All steps of sample and microarray processing were performed according to manufacturer's recommendations. CEL files were generated from DAT files using GCOS software (Affymetrix). Probe set expression estimates were calculated using RNA algorithm in ArrayAssist Lite software version 3.4 (Stratagene, Santa Clara, CA).

Characterization of mRNA integrity

To evaluate mRNA integrity of specimens stored under different conditions, ratios of signal intensities were calculated for probe sets that measure the 3′ and 5′ ends of two genes (GAPDH and ACTB). Because first strand cDNA synthesis uses oligo(dT), RNA degradation can cause reduced signal intensities at the 5′ end of transcripts and therefore can increase 3′:5′ ratios. To evaluate whether certain transcripts from specific genes showed consistent alterations due to storage conditions, significance analysis of microarrays (SAM) was used (Tusher et al. 2001).

Biotech Histochem Downloaded from informahealthcare.com by Dr. G.S. Nettleton on 06/25/14
For personal use only.

Protein analysis by mass spectrometry

Frozen sections from matched pairs from eight cases were cut at 5 µm and mounted on glass microscope slides for histopathological analysis. These samples were selected from various tumor specimens in which aliquots of the same specimen were stored for ≥9 years at either −80° C or in VPLN. The frozen sections of both aliquots of a pair were reviewed by a pathologist to verify that each aliquot was equivalent by microscopic examination, i.e., those that contained approximately the same content and histology of the tumor. Ten micrometer sections then were cut from the equivalent paired samples and mounted for analysis by mass spectrometry. The analysis was blinded concerning which aliquot of each specimen was stored at one or the other temperature. When the 5 µm sections of both aliquots of a pair were equivalent by microscopic examination, e.g., contained approximately the same content of tumor, up to eight 10 µm frozen sections, depending upon the tumor in the respective frozen section, were scraped from the slide, avoiding the OCT, and were lysed with 100 µl of lysis buffer (20 mm Hepes, pH 8.0, 1% Tween 20). The supernatants were separated using a high speed microfuge at 10,000 x g for 10 min Eight pairs of samples of the specimens that had been stored ≥9 years were analyzed (Table 2).

The protein in each lysate supernatant was measured using the Pierce BCA protein assay and an equivalent amount of protein (10 µg) was loaded in triplicate with each of the aliquots loaded randomly on one of the eight sampling spots of an IMAC-3 copper activated metal chip (Bio-Rad, Hercules, CA). Each spot on the chip was analyzed by surfaced enhanced laser absorption/desorption time of flight mass spectrometry (SELDI-TOF-MS, Protein Biosystem II; Bio-Rad). In general, the approach described earlier was used for copper activation and sample loading (Adam et al. 2002, Semmes et al. 2005, McLerran et al. 2008a,b, Grizzle et al. 2005a,b). Specifically, the blinded samples were processed using a Biomek 2000 (Beckman Coulter, Brea, CA) robotic sample preparation platform that diluted the samples and loaded them on the IMAC-3 copper activated surface. The robotic system also spotted sinapinic acid matrix on each sample. A control sample was loaded and analyzed in at least one of the eight wells of each metal chip; locations of cases and controls on chips were chosen randomly to minimize bias (Adam et al. 2002, Semmes et al. 2005, McLerran et al. 2008a,b, Grizzle et al. 2005a,b).

The metal IMAC-3 chips also were read on a MALDI-TOF-MS (Ultraflex III, Brüker Daltronics, Billerica, MA) using an adapter plate made specifically for the Brüker instrument. All samples were prepared according to the manufacturer's instructions (see above). Our method of MALDI-TOF-MS analysis has been reported previously (Kojima et al. 2008). Specifically, 1600 shots were acquired automatically from 2000–100,000 m/z with high filtering set to on, deflector set to 1000 m/z, and detector gain set at 1769 V, using smart beam technology at a single (empirically determined) laser energy, while using a random walk command. Fuzzy acquisition was turned on to avoid summing poor spectra. Flexanalysis then was used to baseline subtract all spectra using a

Table 2. Pairs of surgical specimens stored for at least 9 years and analyzed by mass spectrometry

Case no.	Diagnosis	Condition	Storage period
1A	Langerhans histiocytosis	−80° C	10 years
1B	Langerhans histiocytosis	liquid nitrogen	
2A	ependymoma	−80° C	9 years
2B	ependymoma	liquid nitrogen	
3A	spleen, non-neoplasia	−80° C	11 years
3B	spleen, non-neoplasia	liquid nitrogen	
4A	lymphoma	−80° C	12 years
4B	lymphoma	liquid nitrogen	
5A	hepatoblastoma	−80° C	10 years
5B	hepatoblastoma	liquid nitrogen	
6A	lymph node, follicular hyperplasia	−80° C	11 years
6B	lymph node, follicular hyperplasia	liquid nitrogen	
7A	MPNST	−80° C	11 years
7B	MPNST	liquid nitrogen	
8A	PNET	−80° C	12 years
8B	PNET	liquid nitrogen	

top hat approach followed by a batch text output processing script (written in house), thus allowing further processing to be carried out in MatLab (Mathworks, Natick, MA).

Specimens of lysate also were analyzed using nano-liquid chromatography electrospray ionization tandem mass spectrometry (nLC-ESI-MS/MS) as described earlier (Wang et al. 2010). For these experiments, protein extracts were concentrated and exchanged using equal volumes of 50 mM ammonium bicarbonate three times using 3 K cutoff spin filters (EMD Millipore, Billerica, MA) and digested overnight with trypsin gold (Promega, Madison WI) according to the manufacturer's recommendations. The resulting peptides were diluted to 100 ng/µl in 0.1% formic acid and 5 µl were subjected to nLC-ESI-MS/MS analysis using a ThermoFisher Scientific, Inc., Waltham, MA LTQ-XL ion trap mass spectrometer equipped with a Thermo MicroAS autosampler and Thermo Surveyor HPLC pump, Nanospray source, and Xcalibur 1.4 instrument control (ThermoFisher Scientific, Inc.). Proteins were searched in species-specific subsets of the UniRef database (European Bioinformatics, Cambridge, UK). Tandem mass spectrometry data were converted to mzXML format using instrument-specific conversion software (Institute for Systems Biology, Seattle WA; Fred Hutchinson Cancer Center) and run separately through SEQUEST (ThermoFisher Scientific, Inc.) with a "no enzyme" setting so that non-trypsin cleavage sites were mapped, and also with MASCOT (Matrix Science Inc., Boston MA) using a "strict trypsin" setting so that only trypsin cleavage sites were mapped. ProteoIQ (BioInquire, Athens, GA) was used to combine tandem mass spectrometry database search results to determine thresholds, which identify as many real proteins as possible while encountering a minimal number of false positive protein identifications. The numbers of unique peptides were calculated per sample based on no enzyme and strict trypsin database searches.

Statistical analysis

To evaluate the significance of differences between RNA and protein integrity from samples stored under the two storage conditions, a paired *t*-test was performed. Total RNA yield, RIN, Degradation Factor, and 3′/5′ ratios of GAPDH and ACTB were analyzed for significant differences. Transcripts with the highest susceptibility to storage-induced degradation were identified by paired analysis performed in SAM using a false discovery rate (FDR) <0.12 and running 100 permutations. The list of significant transcripts expressed differentially provided by SAM was used for EASE analysis (Hosack et al. 2003) to identify preferentially affected gene ontology categories. Results of EASE analysis are reported when the EASE score is less than 0.05 after Benjamini correction.

For the MALDI-TOF-MS analysis, the MatLab toolbox was used to align and peak-select mass spectra, thus producing a peak matrix file that then was applied to calculate mean intensities and coefficient of variance. For the LC-ESI-MS data, ProteoIQ (NuSep) was used to incorporate the two most common methods for statistical validation of large proteome datasets; false discovery rate (FDR) calculations combined with peptide and protein probability approaches were used (Keller et al. 2002, Nesvizhskii et al. 2003, Weatherly et al. 2005). The cutoff was selected at less than 1%.

Results

RNA

Microarray analysis was performed and mRNA integrity was assessed by 3′/5′ ratios of GAPDH and ACTB. Neither GAPDH nor ACTB showed significant integrity differences caused by different storage conditions (Table 3).

Based on the assumption that certain transcripts could be especially susceptible to storage-induced RNA degradation, SAM was performed to identify transcripts with significant differences between

Table 3. RNA yield and integrity of specimens after long term storage at −80° C and in VPLN

	−80° C		VPLN		
	Mean	**Standard deviation**	**Mean**	**Standard deviation**	***p* value**
yield	7100 ng	6800 ng	4400 ng	5400 ng	0.006
RIN	5.8	2.8	4.3	3.3	0.0002
DF	39	37	56	42	0.003
3′:5′ GAPDH	2.6	6.2	2.2	5.8	0.9
3′:5′ ACTB	52	49	54	55	0.5

Biotech Histochem Downloaded from informahealthcare.com by Dr. G.S. Nettleton on 06/25/14
For personal use only.

paired samples. All 44 probe sets with the highest significant differences between the groups showed higher signals in the group of samples stored at −80° C compared to those stored in VPLN (Table 4). We conclude that certain transcripts are especially susceptible to storage-induced degradation, which causes signal loss in the VPLN stored samples. Gene Ontology analysis of the 44 transcripts identified by SAM showed significant over-representation of specific biological themes (Table 5). This means that it is very unlikely that the differences between the two storage conditions could have been caused by random variation between samples.

Owing to the unexpected finding that samples stored at −80° C showed greater RNA integrity, we investigated whether removing the samples from storage boxes could be a confounding factor that affects RNA integrity. When samples from a storage box were removed, the entire box was stored for several minutes on dry ice and this could expose

Table 4. Probe sets with significantly lower signals in specimens stored in VPLN compared to −80° C according to SAM analysis

Probe set ID	Gene name
202087_s_at	cathepsin L
209581_at	HRAS-like suppressor 3
211911_x_at	major histocompatibility complex, class I, B
201272_at	aldo-keto reductase family 1, member B1 (aldose reductase)
209612_s_at	alcohol dehydrogenase IB (class I), beta polypeptide
201649_at	ubiquitin-conjugating enzyme E2L 6
208729_x_at	major histocompatibility complex, class I, B
209059_s_at	endothelial differentiation-related factor 1
211991_s_at	major histocompatibility complex, class II, DP alpha 1
202675_at	succinate dehydrogenase complex, subunit B, iron sulfur (Ip)
214864_s_at	glyoxylate reductase/hydroxypyruvate reductase
200725_x_at	ribosomal protein L10
210972_x_at	T cell receptor alpha locus /// T cell receptor alpha constant
206559_x_at	eukaryotic translation elongation factor 1 alpha 1
209036_s_at	malate dehydrogenase 2, NAD (mitochondrial)
211529_x_at	HLA-G histocompatibility antigen, class I, G
211799_x_at	major histocompatibility complex, class I, C
209613_s_at	alcohol dehydrogenase IB (class I), beta polypeptide
208870_x_at	ATP synthase, H+ transporting, mitochondrial F1 complex, gamma polypeptide 1
202201_at	biliverdin reductase B (flavin reductase (NADPH))
201231_s_at	enolase 1, (alpha)
213366_x_at	ATP synthase, H+ transporting, mitochondrial F1 complex, gamma polypeptide 1
202746_at	integral membrane protein 2A
200737_at	phosphoglycerate kinase 1
210460_s_at	proteasome (prosome, macropain) 26S subunit, non-ATPase, 4
212085_at	solute carrier family 25, member 6
201931_at	electron-transfer-flavoprotein, alpha polypeptide (glutaric aciduria II)
200820_at	proteasome (prosome, macropain) 26S subunit, non-ATPase, 8
204599_s_at	mitochondrial ribosomal protein L28
209244_s_at	kinesin family member 1C
217933_s_at	leucine aminopeptidase 3
202474_s_at	host cell factor C1 (VP16-accessory protein)
204806_x_at	major histocompatibility complex, class I, F
218893_at	isochorismatase domain containing 2
200663_at	CD63 antigen (melanoma 1 antigen)
217972_at	coiled-coil-helix-coiled-coil-helix domain containing 3
218232_at	complement component 1, q subcomponent, alpha polypeptide
202343_x_at	cytochrome c oxidase subunit Vb
214836_x_at	HRV Fab N8-VL
217408_at	mitochondrial ribosomal protein S18B
215313_x_at	major histocompatibility complex, class I, A
210547_x_at	islet cell autoantigen 1, 69 kDa
213160_at	dedicator of cytokinesis 2
200752_s_at	calpain 1, (mu/l) large subunit

Biotech Histochem Downloaded from informahealthcare.com by Dr. G.S. Nettleton on 06/25/14
For personal use only.

Table 5. Gene ontology categories over-represented in the 44 probe sets with significantly lower signals in specimens stored at VPLN

System	Gene category	EASE score	Benjamini
GO Biological process	antigen presentation	2×10^{-8}	3×10^{-6}
	antigen processing	2×10^{-8}	3×10^{-6}
	antigen presentation\, endogenous antigen	4×10^{-8}	4×10^{-6}
	antigen processing\, endogenous antigen via MHC class I	6×10^{-8}	5×10^{-6}

the samples to a temporary temperature increase. The biorepository's database was used to determine the number of times that a storage box was moved from VPLN to dry ice because of routine specimen retrieval during the period of sample storage. Neither the number of accessions of a box nor the number of accessions of aliquots from the same sample was related to the loss of the ten most degradation-sensitive transcripts identified by SAM (data not shown).

Protein

The peaks generated from the various aliquots analyzed by SELDI-TOF-MS, which was utilized to assess whole "non-enzyme digested" low molecular weight proteins and peptides, were similar to the equivalent triplicate measurements of each aliquot (Fig. 1). In some cases, the visual analysis of a blinded aliquot stored at −80° C yielded a higher signal to noise ratio for specific features, while this observation was reversed for other features depending on the type of tissue specimen stored in VPLN. We could not identify consistently which storage condition gave the best results for analyzing these samples; however, the spectra obtained from both groups were qualitatively similar and reproducible despite the different conditions and times of storage.

Based on the qualitative results from SELDI-TOF-MS analysis, we initiated a more extensive analysis on the same samples using a high-end MALDI-TOF-MS instrument and a Brüker adapter plate specifically made to fit the SELDI-MS probes. All spectra were compared across each matched pair with 102 consistent features identified with a signal to noise ratio >4 ($n=4$). Similar results were obtained; features within the −80° C group had a coefficient of variation (CV%) = 0.92, and the VPLN group had a CV% = 0.86. Therefore, the two groups were consistent overall. Specifically, comparing the spectra of matched pairs, the majority of peaks were similar within each aliquot of the matched pairs. Some peaks were observed consistently at one

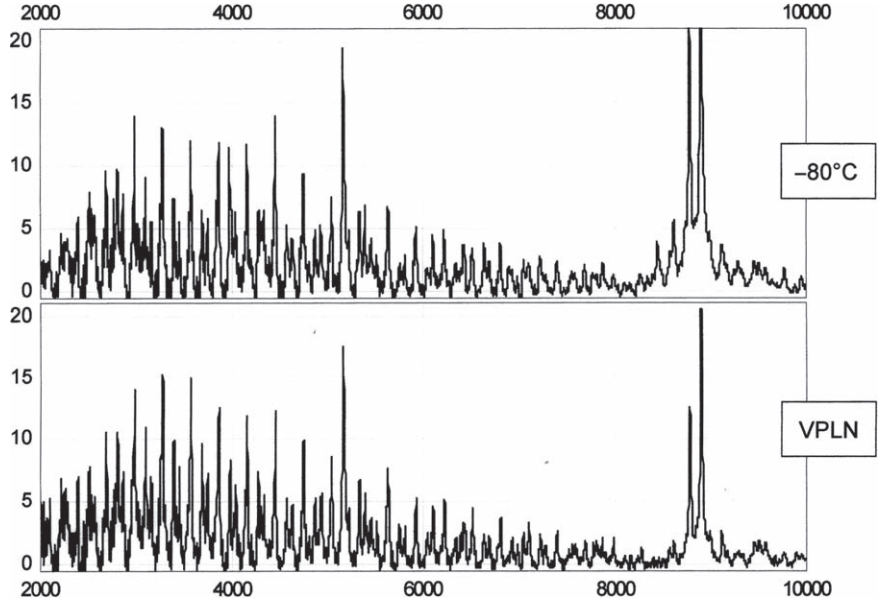

Fig. 1. Spectra from a pair of lysed tissues from separate aliquots of the same human specimen stored under different conditions and for different times at −80° C or in VPLN. The spectra are similar.

Biotech Histochem Downloaded from informahealthcare.com by Dr. G.S. Nettleton on 06/25/14
For personal use only.

storage temperature (e.g., −80º C), but not at the other temperature (e.g., VPLN) and vice versa (i.e., absent at −80° C, but present at VPLN). Thus, an optimal temperature for storage could not be determined using either of these approaches (data not shown).

Finally, using LC-ESI-MS/MS analyses, we compared the protein identification numbers (ID's) of matched pairs and a majority (183 of 239; 77%) was observed consistently in all specimens. The total number of proteins and the number of protein ID's that were independent of each storage group also were similar (total: independent, 210:27 for −80º C and 211:29 for VPLN) (Fig. 2a). All tandem MS/MS spectra generated by the nLC-ESI-MS analysis were matched at the peptide level against all potential "no enzyme" cleavage sites to assess differences that likely are due to either continued endogenous enzymatic degradation or shearing effects caused by the storage method. This value is estimated by assigning MS/MS spectra that match peptide sequences with "strict trypsin" cleavage sites found only at the C-terminal residue of lysine and/or arginine vs. "no enzyme" cleavage sites found at any C- or N- terminal amino acid. While there was a slight increase in all runs using the no enzyme vs. the strict trypsin approach (702 vs. 655, an approximately 7% lower value than 702), there were no consistent differences between the two storage groups (Fig. 2b). Examples of the most abundant proteins identified by mass spectrometry are listed in Table 6.

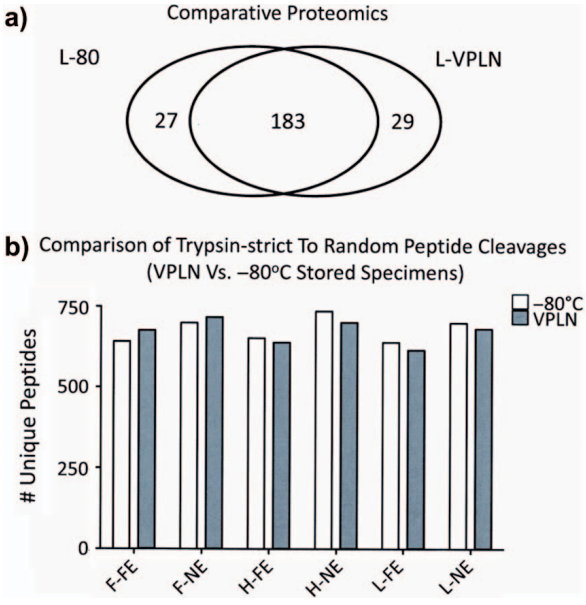

Fig. 2. a) Number of unique peptide ID's generated by LCMS are shown within a strict Venn diagram for the two storage groups (−80° C and VPLN) derived from lymphoma (L) specimens as an example. b) Number of unique peptide identification numbers (ID's) are shown in the figure for each sample for all groups. L, lymphoma; H, hepatoblastoma; F, follicular hyperplasia. Non-neoplastic lymph node comparing full enzyme (FE) and no enzyme (NE) searches in SEQUEST. In this way, we can estimate the number of shearing sites to be expected from freezing thawing or from a less optimal freezing approach.

Discussion

Storage at −80° C and in VPLN are the two most common methods for long term storage of fresh-frozen tissue samples. Little information is available about the relative benefits of these long term storage methods for analysis of RNA or proteins, except that storage near VPLN temperatures is required to maintain long term viability of cells.

Some molecules may be affected by freezing, others by thawing and others by both. Similarly, the duration of long term storage under either condition probably results in molecular changes as indicated by the RIN scores we found for specimens whose average RINs were less than expected for specimens stored for a short time. The freezing and thawing procedures for the two storage methods were equivalent overall. The effects of storage time on RIN were based on paired samples with each tissue specimen of a pair stored for the same time. Thus, the most common difference between each of the paired samples and the differences we observed in RNA and proteins we attribute to storage temperature.

We found that for 49 specimens of various types of tissues and cancers, storage at −80° C maintained at least the same RNA integrity as VPLN storage. For RNA yield and total RNA integrity, −80° C storage provided significantly better results than VPLN storage. For 37 specimens analyzed by expression profiling, mRNA integrity measured by 3′:5′ ratios of GAPDH and ACTB showed no significant differences; by contrast, SAM showed that a number of transcripts seemed to be especially susceptible to degradation in samples stored by VPLN. These transcripts were significantly lower in samples stored in VPLN compared to storage at −80° C. Transcripts that are highly sensitive to VPLN storage frequently are involved in antigen presentation and processing, which suggests that these transcripts may be useful for assessing storage-induced RNA degradation.

With the development of real-time qualitative PCR (RT-Q-PCR), the effects of degradation of RNA may be minimized if short amplicons (≤100 bp) are used. Using this technology, gene expression even in paraffin blocks can be analyzed reliably (Steg

Biotech Histochem Downloaded from informahealthcare.com by Dr. G.S. Nettleton on 06/25/14
For personal use only.

Biotech Histochem Downloaded from informahealthcare.com by Dr. G.S. Nettleton on 06/25/14
For personal use only.

Table 6. Twenty-six most abundant proteins evaluated in the LC-ESI-MS-MS study of −80° C. VPLN storage for three specimens

UniRef100 ID	Sequence name	Protein weight (kDa)	No. unique peptides	H/ VPLN	H/ −80C	%CV	L/ VPLN	L/ −80C	%CV	S/ VPLN	S/ −80C	%CV
B4DMF5	glutamate dehydrogenase 1	56.55	10	28.4	34.2	0.00	2.5	0.0	0.00	0.0	0.0	0.00
B3KQT2	Protein disulfide-isomerase A3	54.85	15	22.2	26.8	18.71	10.1	7.0	35.87	8.3	7.8	6.71
B3KML9	tubulin beta-2C chain	44.56	10	8.7	9.8	12.06	11.3	12.0	5.92	8.3	11.7	33.52
P10809	60 kDa heat shock protein	61.00	20	50.7	61.0	18.47	18.9	12.0	44.46	2.1	2.6	21.84
P11021	78 kDa glucose-regulated protein	72.27	25	64.3	63.4	1.32	18.9	19.0	0.74	10.4	22.0	71.85
P06733	alpha-enolase	47.12	25	33.4	40.2	18.70	44.0	42.0	4.65	14.6	16.9	14.65
B3VL17	beta globin	11.24	11	106.3	80.5	27.61	30.2	45.0	39.46	150.7	132.2	13.06
A8K4K6	disulfide isomerase family A, member 4	72.80	12	22.2	8.5	0.00	0.0	1.0	0.00	0.0	0.0	0.00
P14625	endoplasmin	92.39	25	34.6	45.1	26.39	15.1	14.0	7.49	12.5	13.0	3.85
P04406	glyceraldehyde-3-phosphate dehydrogenase	36.01	13	9.9	23.2	80.34	31.4	42.0	28.79	32.2	25.9	21.63
P11142	heat shock cognate 71 kDa protein	70.84	20	38.3	42.7	10.79	37.7	31.0	19.53	20.8	31.1	39.80
P07900	heat shock protein HSP 90-alpha	84.59	15	40.8	28.1	36.99	16.3	22.0	29.53	13.5	15.6	14.10
P08238	heat shock protein HSP 90-beta	83.19	16	48.2	39.0	21.03	25.1	26.0	3.36	9.4	13.0	32.26
P69905	hemoglobin alpha	15.23	10	70.4	48.8	36.32	11.3	30.0	90.49	139.3	105.0	28.06
Q3LR79	hemoglobin beta	11.46	10	60.6	54.9	9.82	17.6	31.0	55.14	69.6	51.9	29.27
P02042	hemoglobin subunit delta	16.03	12	64.3	46.3	32.39	10.1	20.0	66.13	110.2	106.3	3.58
P68871	LVV-hemorphin-7	15.97	16	116.2	93.9	21.19	32.7	55.0	50.88	189.2	159.5	17.04
Q06830	peroxiredoxin-1	22.08	13	2.5	8.5	110.26	16.3	11.0	39.06	9.4	9.1	3.04
P00558	phosphoglycerate kinase 1	44.57	11	11.1	7.3	41.21	13.8	14.0	1.22	5.2	13.0	85.46
P13796	plastin-2	70.23	11	0.0	0.0	0.00	18.9	15.0	22.80	13.5	14.3	5.40
P14618	pyruvate kinase isozymes M1/M2	57.88	16	1.2	3.7	98.78	23.9	24.0	0.46	11.4	2.6	126.11
Q9Y490	talin-1	269.58	13	0.0	0.0	0.00	1.3	3.0	81.69	16.6	14.3	15.34
P67936	tropomyosin alpha-4 chain	28.49	13	14.8	13.4	10.06	6.3	20.0	104.30	19.8	16.9	15.85
P23381	tryptophanyl-tRNA synthetase	53.11	11	0.0	0.0	0.00	0.0	15.0	200.00	7.3	13.0	56.13
P07437	tubulin beta chain	49.62	17	16.1	20.7	25.39	15.1	24.0	45.59	22.9	18.2	23.01
P08670	vimentin	53.60	24	44.5	37.8	16.24	41.5	48.0	14.55	39.5	50.6	24.56
				sum = 909.4	837.8	25.93 avg. % rsd	470.2	583.0	38.16 avg. % rsd	936.6	866.0	27.16 avg. % rsd

H, hepatoblastoma; LP, lymphoma; S, non-neoplastic spleen; rsd, relative standard deviation.

et al. 2006, 2007). Use of RT-Q-PCR also reduces some concern about long term storage of tissues below −80° C.

We reported earlier that multiple freeze-thaw cycles cause degradation of proteins in samples of serum. We demonstrated also that storage at −80° C for 18 months does not cause significant degradation of many proteins; however, storage of serum samples at −20° C for more than 6 months does cause significant protein degradation (Grizzle et al. 2005a,b). We have shown here that in the absence of thawing, there were no appreciable differences in protein integrity between the two storage methods. While these approaches to mass spectrometry do not evaluate proteins and peptides that are present at low concentrations, for most of the proteins we evaluated, there were no differences between the two storage temperatures; however, it should be emphasized that the proteins analyzed by SELDI-MS, MALDI-MS, and LC-ESI-MS/MS represent only a sample of some of the more abundant proteins of the proteome. Our study was limited to global low resolution studies in which the amounts of protein were small and the resources available for analysis were limited; therefore, specific proteins that were not observed may be more or less susceptible to storage conditions.

The effects of storage temperature on human tissue have not been studied previously to the extent that we present here and our results are informative with regard to the lack of major changes in the most abundant proteins. There is no reason to expect that changes during storage of more abundant proteins do not mirror those of less abundant proteins. Together with the RNA studies, our results suggest that more extensive, high resolution studies are warranted. It is important that most unique proteins identified by mass spectrometry in each member of the paired samples were the same. A relatively few unique proteins were not detected in one of the storage conditions compared to the other storage condition (Fig. 1). Neither method of storage was clearly better than the other with regard to preserving specific proteins (Table 6).

Our results are surprising in view of our current understanding and assumptions regarding temperature and biospecimen integrity. Theoretically, samples stored in VPLN should be below the glass transition temperature of water and no enzymatic or hydrolytic breakdown of RNA or protein should occur. We currently have no hypothesis about why VPLN storage does not conserve RNA integrity as well as −80° C storage. Some of the specimens stored in VPLN were removed from the freezer more frequently for distribution of specimens to researchers and this could have affected RNA integrity adversely if the specimens were warmed above the glass transition phase for short periods of time. If this hypothesis were true, however, one would expect that samples that were moved more frequently would show a greater degree of RNA degradation, but we found no such correlation in our cohort. There is controversy concerning the exact T_g of pure water (Giovambattista et al. 2004) and the T_g of the water phase of mammalian tissues is unknown; however, enzymatic reactions are thought to continue at −80° C.

We conclude that the long term storage of fresh-frozen human tissue specimens in mechanical −80°C freezers preserves at least the same RNA and protein quality as specimens stored in VPLN.

Acknowledgements

Drs. Ramirez and Grizzle are co-senior authors on this manuscript. Supported by all the individual grants of the Cooperative Human Tissue Network (CHTN) and the University of Alabama at Birmingham Mass Spectrometry/Proteomics (MSP) and Tissue Procurement Shared Facilities of the University of Alabama at Birmingham Comprehensive Cancer Center.

Dedication

This manuscript is dedicated to Dr. Steven J. Qualman, who is deceased. Without Steve's vision and leadership, this manuscript would not have been possible. David L. Newsom, who is deceased, also contributed to this manuscript.

Declaration of interest: The authors report no conflicts of interest. The authors alone are responsible for its contents.

References

Adam BL, Qu Y, Davis JW, Ward MD, Clements MA, Cazares LH, Semmes OJ, Schellhammer PF, Yasui Y, Feng Z, Wright GL Jr (2002) Serum protein fingerprinting coupled with a pattern-matching algorithm distinguishes prostate cancer from benign prostate hyperplasia and healthy men. *Cancer Res.* 62: 3609–3614.

Auer H, Lyianarachchi S, Newsom D, Klisovic MI, Marcucci G, Kornacker K (2003) Chipping away at the chip bias: RNA degradation in microarray analysis. *Nat. Genet.* 35: 292–293.

Giovambattista N, Angell CA, Sciortino F, Stanley HE (2004) Glass-transition temperature of water: a simulation study. *Am. Phys. Soc.* 93: 047801-1-047801-4.

Biotech Histochem Downloaded from informahealthcare.com by Dr. G.S. Nettleton on 06/25/14
For personal use only.

Grizzle WE, Semmes OJ, Bigbee W, Zhu L, Malik G, Oelschlager DK, Manne B, Manne U (2005a) The need for the review and understanding of SELDI/MALDI mass spectroscopy data prior to analysis. *Cancer Informat.* 1: 86–97.

Grizzle WE, Semmes OJ, Bigbee WL, Malik G, Miller E, Manne B, Oelschalger DK, Zhu L, Manne U (2005b) Use of mass spectrographic methods to identify disease processes. In: Patrinos G, Ansorg W, Eds., *Molecular Diagnostics,* Chapter 17, Academic Press/ Elsevier, Waltham, MA. pp. 211–222.

Hosack DA, Dennis G Jr, Sherman BT, Lane HC, Lempicki RA (2003) Identifying biological themes within lists of genes with EASE. *Genome Biol*. 4:R70. Epub 2003 Sep 11.

Keller A, Nesvizhskii AI, Kolker E, Aebersold R (2002) Empirical statistical model to estimate the accuracy of peptide identifications made by MS/MS and database search. *Anal. Chem.* 74: 5383–5392.

Kojima K, Asmellash S, Klug CA, Grizzle WE, Mobley JA, Christein JD (2008) Applying proteomic-based biomarker tools for the accurate diagnosis of pancreatic cancer: *J. Gastrointest. Surg.* July; DOI 10.1007/ s11605-008-0632-6.

McLerran D, Grizzle WE, Feng Z, Thompson IM, Bigbee WL, Cazares LH, Chan DW, Dahlgren J, Diaz J, Kagan J, Lin DW, Malik G, Oelschlager D, Partin A, Randolph TW, Sokoll L, Srivastava S, Srivastava S, Thornquist M, Troyer D, Wright GL, Zhang Z, Zhu L, Semmes OJ (2008a) SELDI-TOF MS whole serum proteomic profiling with IMAC surface does not reliably detect prostate cancer. *Clin. Chem*. 54: 53–60.

McLerran D, Grizzle WE, Feng Z, Bigbee WL, Banez LL, Cazares LH, Chan DW, Diaz J, Izbicka E, Kagan J, Malehorn DE, Malik G, Oelschlager D, Partin A, Randolph T, Rosenzweig N, Srivastava S, Srivastava S, Thompson IM, Thornquist M, Troyer D, Yasui Y, Zhang Z, Zhu L, Semmes OJ (2008b) Analytical validation of serum proteomic profiling for diagnosis of prostate cancer: Sources of sample bias. *Clin. Chem.* 54: 44–52.

Nesvizhskii AI, Keller A, Kolker E, Aebersold R (2003) A statistical model for identifying proteins by tandem mass spectrometry. *Anal. Chem.* 75: 4646–4658.

Semmes OJ, Feng Z, Adam B-L, Banez LL, Bigbee WL, Campos D, Cazares LH, Chan DW, Grizzle WE, Izbicka E, Kagan J, Malik G, McLerran D, Moul JW, Partin A, Prasanna P, Rosenzweig J, Sokoll LJ, Srivastava S, Srivastava S, Thompson I, Welsh MJ, White N, Winget M, Yasui Y, Zhang Z, Zhu L (2005) Evaluation of serum protein profiling by surface-enhanced laser desorption/ionization time-of-flight mass spectrometry for the detection of prostate cancer: I. Assessment of platform reproducibility. *Clin. Chem.* 51: 102–112.

Steg A, Wang W, Blanquicett C, Grunda JM, Eltoum IA, Wang K, Buchsbaum DJ, Vickers SM, Russo S, Diasio RB, Frost AR, Grizzle WE, Johnson MR (2006) Multiple gene expression analyses in paraffin-embedded tissues by Taqman low density array: application to Hedgehog and Wnt pathway analysis in ovarian endometrioid adenocarcinoma. *J. Mol. Diagn.* 8: 76–83.

Steg A, Vickers SM, Eloubeidi M, Wang W, Eltoum IA, Grizzle WE, Saif MW, Lobuglio AF, Frost AR, Johnson MR (2007) Hedgehog pathway expression in heterogeneous pancreatic adenocarcinoma: implications for the molecular analysis of clinically available biopsies. *Diagn. Mol. Pathol.* 16: 229–237.

Tusher VG, Tibshirani R, Chu G (2001) Significance analysis of microarrays applied to the ionizing radiation response. *Proc. Natl. Acad. Sci. USA* 98: 5116–5121.

Wang L, Clark ME, Crossman DK, Kojima K, Messinger JD, Mobley JA, Curcio CA (2010) Abundant lipid and protein components of drusen. *PLoS ONE* 5: e10329. doi:10.1371/journal.pone.0010329.

Weatherly DB, Atwood JA III, Minning TA, Cavola C, Tarleton RL, Orlando R (2005) A heuristic method for assigning a false-discovery rate for protein identifications from Mascot database search results. *Mol. Cell. Proteom.* 4: 762–772.

Biotech Histochem Downloaded from informahealthcare.com by Dr. G.S. Nettleton on 06/25/14
For personal use only.

Abstract for the EAU Section of Urological Research (ESUR) meeting in October 2014 in Glascow Scotland

Performance of an epigenetic assay to predict prostate cancer aggressiveness: Comparing Gleason score and NCCN risk categories

Van Neste L.[1], Van Criekinge W.[2], Bigley J.[3], Grizzle W.E.[4], Adams G.W.[5], Kearney G.P.[6], Gaston S.M[7]

[1]Maastricht University Medical Center, Dept. Of Pathology, Maastricht, Netherlands, The,[2]Ghent University, Dept. of Mathematical Modeling, Statistics and Bio-Informatics, Ghent, Belgium, [3]MDxHealth, Clinical Affairs, Irvine, United States, [4]University of Alabama At Birmingham, Dept. of Pathology, Birmingham, United States, [5]Urology Centers of Alabama, Clinical Research Department, Birmingham, United States, [6]Harvard Medical School, Dept. of Surgery, Boston, United States, [7]Tufts University School of Medicine and Tufts Medical Center, Dept. of Pathology, Boston, United States

Introduction & Objectives: Prostate cancer (PCa) remains the most frequent cancer in men in the western world, accounting for roughly 25% of all new cases. Because of available screening techniques, particularly by measuring serum prostate-specific antigen (PSA) levels, and treatment options, PCa-specific death represents only 10% of all cancer-related deaths. Treatment options are typically determined by the expected disease prognosis, mainly guided by Gleason scoring of a cancer-positive biopsy. Since only a small part of the prostate, typically less than 1%, is examined through histopathology prior to treatment and because of fear for overtreatment and associated risks, more accurate and objective prognosis is needed to improve patient management.

Material & Methods: One hundred and two men underwent a 12-core prostate biopsy under routine clinical practice. All patient data was anonymized and institutional review board approval was obtained. No evidence of PCa was found in 20 (20%) patients. For 46 (45%) men, the highest observed Gleason score (GS) was 3+3, making these potential candidates for active surveillance programs. The remaining patients all had higher-grade disease, of which 26 (25%) with GS 3+4, 8 (8%) with GS 4+3, 1 (1%) with GS 7 and 1 (1%) with GS 4+4. All individual biopsy cores were epigenetically profiled using a quantitative methylation-specific PCR assay determining the DNA-methylation status of three markers, i.e. GSTP1, RASSF1 and APC, previously shown to be associated with PCa development.

Results: Unsupervised hierarchical clustering was performed identifying a group of men whose biopsies were highly methylated for these three markers, of which ~75% had higher-grade disease. High-grade PCa also appeared to exhibit a field effect, since the correlation between increased methylation signals and higher GS prevailed even when those cores with GS ≥ 7 were not taken into account. A logistic regression model including the epigenetic signature, PSA and age indicated that the overall average GSTP1 methylation signal was the most significant risk factor. Patients were also stratified according to the national comprehensive cancer network (NCCN) risk categories. The central role for GSTP1 was confirmed for the NCCN risk categories intermediate (n=27) and high (n=1). When the NCCN low risk (n=8) group was also included in the aggressive PCa category, RASSF1 was identified as the best predictor. Methylated signal cutoffs were determined for the two most promising genes, GSTP1 and RASSF1, showing that higher-grade tumors were associated with more positive cores.

Conclusions: Epigenetic profiling of GSTP1, RASSF1 and APC of individual biopsy cores could be used to evaluate PCa aggressiveness in an objective manner and potentially influence patient management. Long-term follow-up is required to show that these correlations are independent of Gleason patterns or NCCN risk categories.